JOURNAL OF PETROLOGY | VOLUME 41 | NUMBER 4 | PAGES 511–543 | 2000

Modelling Diverse Processes in the Petrogenesis of a Composite Batholith: the Central Bohemian Pluton, Central European Hercynides

VOJTĚCH JANOUŠEK[1,2]*, D. R. BOWES[1], GRAEME ROGERS[2], COLIN M. FARROW[1] AND EMIL JELÍNEK[3]

[1]DIVISION OF EARTH SCIENCES, UNIVERSITY OF GLASGOW, GLASGOW G12 8QQ, UK

[2]ISOTOPE GEOSCIENCES UNIT, SCOTTISH UNIVERSITIES RESEARCH AND REACTOR CENTRE, EAST KILBRIDE, GLASGOW G75 0QF, UK

[3]DEPARTMENT OF GEOCHEMISTRY, CHARLES UNIVERSITY, ALBERTOV 6, 128 43 PRAGUE 2, CZECH REPUBLIC

RECEIVED OCTOBER 28, 1998; REVISED TYPESCRIPT ACCEPTED SEPTEMBER 27, 1999

The multiple intrusions making up the Central Bohemian Pluton in the Central European Hercynides have petrographic and geochemical features consistent with the presence of four main granitoid suites. Major-element, trace-element and Sr–Nd isotopic compositions are used to model their petrogenesis. Partial melting of metabasic rocks or of a CHUR-like mantle source are interpreted to have produced melts parental to the most primitive calc-alkaline Sázava suite. Interaction of basic with more acidic magmas followed by extensive amphibole–plagioclase-dominated fractionation accounts for the production of trondhjemites. Alternatively, the trondhjemites correspond to small-degree melts of a metabasic source. AFC (assimilation–fractional crystallization) modelling with a paragneiss as a contaminant and increasing D_{Nd} *values simulates the characteristics of the Blatná suite. Closed-system fractionation of strongly enriched mantle-derived magmas or their interaction with leucogranitic melts is deduced for the petrogenesis of the shoshonitic Čertovo břemeno suite. Partial melting of a metasedimentary source, followed by K-feldspar-dominated fractionation, accounts for the granites of the Říčany suite. The progression from relatively primitive calc-alkaline granitoids towards evolved, K-rich calc-alkaline and shoshonitic rocks is interpreted to reflect the increasing enriched mantle input in the petrogenesis of the later suites. The evidence for Hercynian subduction is equivocal and the mantle enrichment could have been significantly older.*

KEY WORDS: *batholith; granitoids; Hercynides; petrogenesis*

INTRODUCTION

The 3200 km^2 Central Bohemian Pluton (CBP; Fig. 1) in the Czech Republic is one of the largest composite granitoid complexes in the Central European Hercynides. What makes it special is its great compositional variation, ranging from gabbro, diorite, quartz monzonite, tonalite, trondhjemite and granodiorite to granite (Holub *et al.*, 1997*b*). Melanocratic K-rich syenites to melagranites also occur, with several of the more mafic types corresponding to rocks of the durbachite suite (Holub, 1989, 1997). As a consequence, the CBP offers an excellent opportunity, within a restricted geographical area, for assessing the nature of the petrogenetic processes that give rise to a composite batholith, particularly in the context of the Central European Hercynides.

The aim of this study is to characterize the whole-rock major- and trace-element geochemistry of some of the larger intrusions covering much of both the overall timespan of the CBP and the range of geochemical variation, complementing published Sr–Nd isotopic data (Janoušek *et al.*, 1995). Geochemical criteria are established for distinguishing cognate groups of intrusions and a petrogenetic model is formulated to account for the observed variations. This model, based upon combined modelling of major elements, trace elements and Sr–Nd isotopes,

*Corresponding author. Present address: Czech Geological Survey, Klárov 3/131, 118 21 Prague 1, Czech Republic. Telephone: +(4202) 581 87 40, ext. 308. Fax: +(4202) 581 8748. e-mail: janousek@cgu.cz

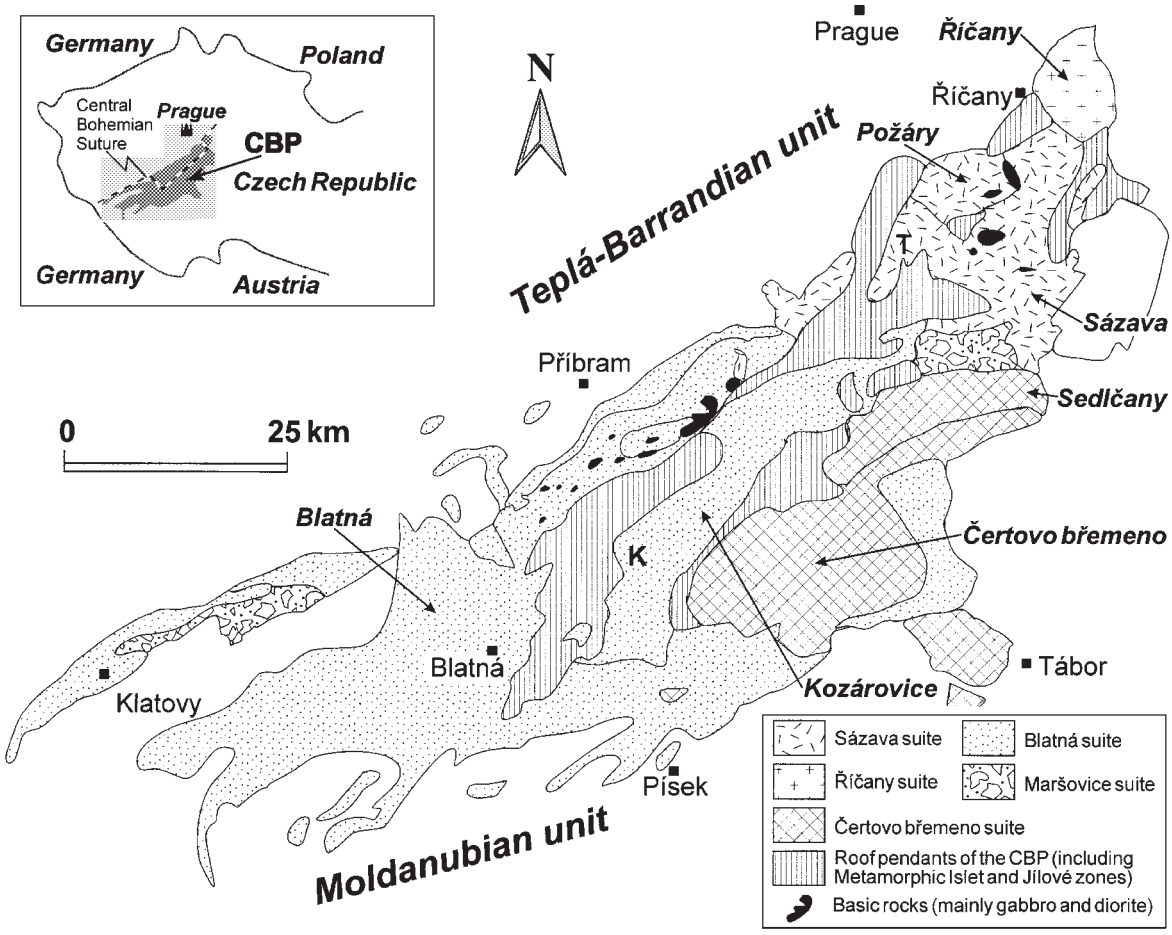

Fig. 1. Schematic map of the Central Bohemian Pluton (CBP) [based partly on Mísař *et al.* (1983) and Holub *et al.* (1997*b*)] showing the Říčany, Požáry, Sázava, Blatná, Kozárovice, Sedlčany and Čertovo břemeno intrusions of the four main granitoid suites (Sázava, Blatná, Čertovo břemeno and Říčany suites; named after the most prominent intrusion) and the Maršovice suite (not included in the petrogenetic study); T (Teletín quartz diorite) and K (Kozárovice quartz monzonite) show positions of small intrusions referred to in the text.

allows constraints to be placed on the possible sources and processes that were involved in the genesis of the granitoid rocks of the CBP.

REGIONAL SETTING OF THE CBP

The CBP has intruded a major NE–SW trending tectonic zone, the Central Bohemian Suture, which forms the boundary between the Teplá–Barrandian unit (mainly weakly metamorphosed or unmetamorphosed Upper Proterozoic–mid-Devonian sediments) in the NW and the Moldanubian unit (a tectonic assemblage of medium- to high-grade metamorphic rocks of early Proterozoic to early Palaeozoic age) in the SE (Fig. 1) (e.g. Blížkovský *et al.*, 1992). This tectonic zone may represent a ramp region in a major shear zone, which could have exerted a significant control on the emplacement of the CBP (Košler *et al.*, 1995).

Roof pendants within the batholith include a belt of Proterozoic to Lower Palaeozoic (to mid-Devonian: Chaloupský *et al.*, 1995) metasediments and basic volcanic rocks (Metamorphic Islet Zone), tonalitic–granodioritic orthogneisses, which are tectonothermally modified mid–late Devonian calc-alkaline granitoids (Mirotice, Staré Sedlo and Lašovice complexes: Košler, 1993; Košler *et al.*, 1993) and Upper Proterozoic volcanic and volcanogenic rocks (Jílové zone). The contacts of the CBP with both the roof pendants and the Teplá–Barrandian unit are sharp, with a strong thermal metamorphism. In many places the Moldanubian unit adjacent to the CBP has been intensely migmatized.

Mainly on the basis of their distinct appearance in the field, more than 20 major intrusions or 'rock types' have been recognized in the CBP. In addition, dozens of other names exist, either for minor intrusions or simply as a continuation of historical tradition. Most of the rocks,

however, fall into several distinct groups or suites on the basis of their petrography and geochemical characteristics. An approach that involves only a limited number of suites both helps in genetic interpretations and reduces the plethora of names for the intrusions. Such an approach is analogous to that used in the Lachlan Fold Belt of eastern Australia (e.g. White & Chappell, 1988) with each suite having its own identity in terms of relative age, modal and chemical compositions, textures, enclave and dyke-swarm populations. The classification of the CBP adopted here follows that of Janoušek (1994) and Janoušek *et al.* (1995) slightly modified from Holub (1992) (Fig. 1; see Holub *et al.*, 1997*b*), with the following main suites (named after the most prominent intrusion): Sázava, Blatná, Čertovo břemeno and Říčany. Neither rocks of the Maršovice suite, regionally rather insignificant peraluminous S-type granitoids (Holub *et al.*, 1997*b*), nor small leucogranitic bodies distributed mainly in the eastern CBP, were investigated. On the other hand, data are presented for minette dykes, which cut mainly rocks of the Blatná suite: their petrographic and geochemical characters are consistent with being the most primitive members of the Čertovo břemeno suite.

Geological evidence (Janoušek *et al.*, 1995; Holub *et al.*, 1997*b*, and references therein) points to a late Devonian–early Carboniferous age for most of the CBP. This is supported by Pb–Pb single-zircon evaporation ages for the Sázava (349 ± 12 Ma), Požáry (351 ± 11 Ma; both Sázava suite), Blatná (346 ± 10 Ma) and Čertovo břemeno (343 ± 6 Ma) intrusions (Holub *et al.*, 1997*a*) as well as by conventional U–Pb zircon ages for the Klatovy (349^{+6}_{-4}) Ma and Nýrsko (341 ± 2 Ma) intrusions (both Blatná suite; Dörr *et al.*, 1998). $^{40}Ar/^{39}Ar$ biotite ages of 339 ± 10 Ma (Klatovy intrusion: Dörr *et al.*, 1998), 342 ± 8 Ma (Nýrsko intrusion: Dörr *et al.*, 1998), 336 Ma (Čertovo břemeno intrusion: Matte *et al.*, 1990) and 336 ± 3·5 Ma (Říčany intrusion: H. Maluski, personal communication, 1995) represent cooling ages.

PETROGRAPHY

Sázava suite

Much of the northern CBP is formed by the irregularly shaped Sázava intrusion (Fig. 1) composed of amphibole–biotite to biotite–amphibole quartz diorite, tonalite and granodiorite. It contains about 40–75% plagioclase, 2–35% magnesio-hornblende, 15–35% quartz, ~10% biotite and 0–12% K-feldspar; common accessory minerals include titanite, apatite, zircon, allanite, epidote and opaque minerals [see Kodymová & Vejnar (1974) for a detailed account of accessory minerals in all major intrusions of the CBP]. Although the typical Sázava plagioclase is unzoned and of andesine composition, some crystals show discontinuous zoning with cores of andesine–labradorite, and rims of sodic andesine. The intrusion contains abundant mafic microgranular enclaves (MME) and much scarcer, mainly metabasic, country-rock xenoliths. This, coupled with the absence of surmicaceous enclaves (Didier & Barbarin, 1991), suggests a negligible metasedimentary but a significant basic igneous input.

At the western margin of the Sázava intrusion there are small bodies of fine-grained quartz diorite with plagioclase megacrysts (Teletín quartz diorite). This unit contains acicular apatites, oikocrysts of quartz and K-feldspar [similar to textures described by Vernon (1991)] and zoned amphiboles with pargasite and magnesio-hastingsite cores, resorbed and overgrown by magnesio-hornblende similar in composition to the amphiboles common in the adjacent Sázava intrusion. Plagioclase is often discontinuously zoned, with resorbed bytownite–anorthite cores overgrown by andesine–labradorite rims, the latter corresponding to the unzoned plagioclase of the matrix. Such mineralogical features are consistent with a hybrid origin of the body (Janoušek *et al.*, 1997*a*). Other numerous bodies of pyroxene–amphibole gabbro, some with olivine, together with less frequent gabbrodiorite, (quartz) diorite and rare hornblendite are also associated with the Sázava intrusion.

The Požáry intrusion is composed of biotite trondhjemite and leucocratic quartz diorite (55–70% plagioclase, 20–30% quartz, 5% K-feldspar, 4–8% biotite, typically without amphibole). It is poor in apatite and zircon; the main accessory mineral is magnetite. The intrusion frequently contains mantled oligoclase–andesine megacrysts, whose rims have the same composition (sodic andesine) as the unzoned plagioclase of the matrix. Enclaves are generally sparse; the numbers of MME and metasedimentary xenoliths increase towards the contacts with the Sázava intrusion and the Teplá–Barrandian unit, respectively.

Blatná suite

Granodiorites predominate in the central part of the CBP. The elongate, NE-trending Kozárovice intrusion is formed by biotite–amphibole to amphibole–biotite granodiorite (30–45% plagioclase, 10–30% K-feldspar, 10–20% quartz, 10–20% biotite and up to 20% amphibole). K-feldspar phenocrysts vary in abundance, being most numerous in the central part of the body. Apatite, titanite, zircon and opaque minerals are common accessories. The intrusion contains abundant enclaves, including country-rock xenoliths (hornfels, amphibolite, calc-silicates), MME and surmicaceous enclaves. Some of the large bodies of amphibole ± pyroxene ± quartz monzonite–monzogabbro associated with the Blatná suite show evidence for interaction with the surrounding granodiorite (such as quenched apatites, mantled plagioclases

and resorbed biotites within mainly euhedral amphiboles) indicating that the magmas that crystallized to form the monzonitic rocks and granodiorites were contemporaneous and interacted with each other (e.g. Kozárovice quartz monzonite: Janoušek, 1994; Janoušek *et al.*, 1997*a*).

The amphibole–biotite (common mainly at the margins) to biotite (common in the centre of the intrusion) granodiorite of the Blatná intrusion contains 20–35% quartz, 25–45% plagioclase, 5–30% K-feldspar, 15–25% biotite and up to 5% amphibole, with accessory apatite, zircon, titanite, allanite and opaque minerals. The granodiorite is either equigranular or contains a minor proportion of K-feldspar phenocrysts. In the southern part of the intrusion, there is a more mafic facies which has a strong planar fabric (termed the Červená type). The MME and surmicaceous enclaves are generally common but less so in the amphibole-poor granodiorites, which occur mainly in the central part of the intrusion. Country-rock xenoliths (mainly migmatitic and biotite paragneisses, and, more rarely, carbonate rocks and orthogneisses) are also less frequent in the biotite facies, but show a marked increase in number towards roof pendants and the Moldanubian unit.

Plagioclase in the Kozárovice and Blatná intrusions is mainly normally zoned andesine. Less frequently it has labradorite cores or spikes that may point to interaction with basic magma (see Janoušek *et al.*, 1997*a*).

Čertovo břemeno suite

The NE-trending elongate Sedlčany intrusion comprises porphyritic amphibole–biotite to biotite granite (20–40% quartz, 20–35% plagioclase, 8–40% K-feldspar, 15–25% biotite, and up to 4% amphibole). The most prominent accessory minerals are apatite, zircon, titanite, allanite and opaque minerals. The plagioclase is a relatively homogeneous andesine, with rare oligoclase rims and fracture infillings. Plagioclase crystals enclosed by K-feldspar phenocrysts are usually overgrown by a thin rim of exsolved albite probably of subsolidus origin. Metasedimentary xenoliths, mainly of biotite hornfels, paragneiss, quartz and calc-silicate rock, become more abundant in the western and southwestern parts. MME are also common but surmicaceous enclaves are considerably rarer.

The Čertovo břemeno intrusion is composed of porphyritic amphibole–biotite melagranite and melasyenite resembling the generally coeval K-rich magmatic rocks of the Black Forest, Germany (durbachites; Holub, 1989, 1997). A roughly circular body of biotite–pyroxene syenite to melagranite (with hypersthene and clinopyroxene)—the Tábor syenite—occurs further to the south (Fig. 1).

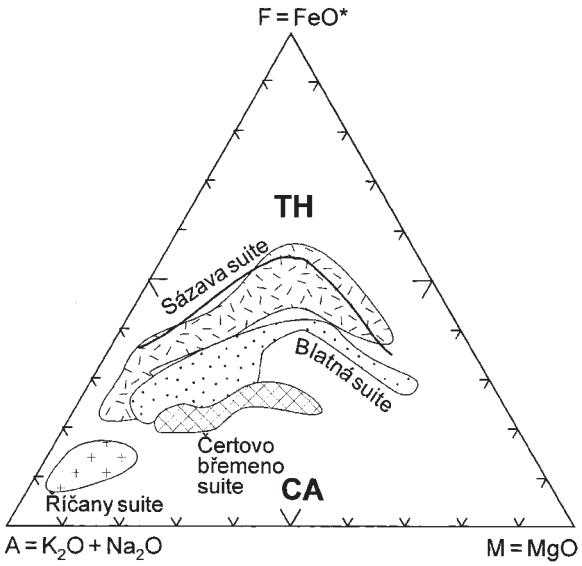

Fig. 2. AFM diagram showing fields for the four main geochemical suites of the CBP plotting below the line dividing tholeiitic (above; TH) and calc-alkaline (below; CA) domains after Irvine & Baragar (1971).

Říčany suite

The Říčany intrusion in the northernmost part of the CBP (Janoušek *et al.*, 1997*c*) comprises a porphyritic biotite granite (~35% K-feldspar, 30% plagioclase, 30% quartz and 5% biotite) with a variable but minor proportion of muscovite (<2%). Apatite and opaque minerals are common accessories; zircon is rarer. The plagioclase is mainly oligoclase; that within K-feldspar phenocrysts has been overgrown by exsolved albite. Various types of enclaves, including MME, surmicaceous enclaves and metasedimentary xenoliths (the latter mainly close to the contact with the Teplá–Barrandian unit) are abundant.

WHOLE-ROCK GEOCHEMISTRY

Major elements

The major-element characteristics of the individual intrusions of the CBP and their grouping into cogenetic suites have recently been reviewed by Holub (1992) and Holub *et al.* (1997*b*). Consequently, the major-element data are discussed only briefly here.

In the AFM diagram (Fig. 2), four distinct groups can be distinguished, with each of the Sázava, Blatná and Čertovo břemeno suites forming a progressively shallower calc-alkaline trend and the Říčany suite plotting close to the A apex. In a SiO_2–K_2O plot (Fig. 3), the relatively low potassium content designates the Sázava suite as being largely calc-alkaline, whereas the Blatná suite is high-K calc-alkaline and both the Čertovo břemeno and Říčany suites, together with the monzonitic rocks of the Blatná suite, are shoshonitic in character.

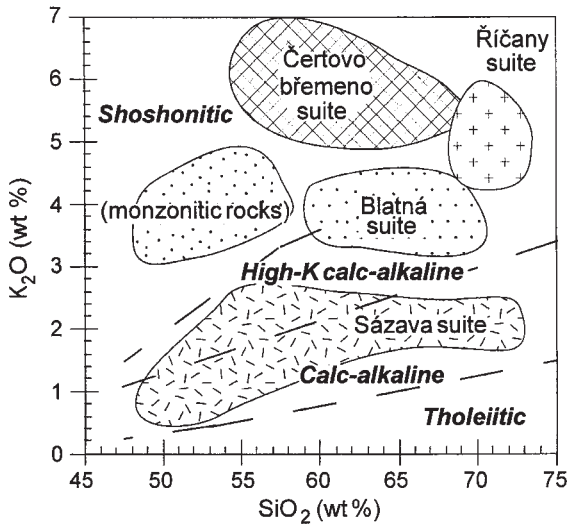

Fig. 3. SiO_2 vs K_2O plot for the four main suites of the Central Bohemian Pluton; the discrimination boundaries between the tholeiitic, calc-alkaline, high-K calc-alkaline and shoshonitic rocks are those of Peccerillo & Taylor (1976).

In terms of alumina saturation (Table 1), some rocks of the Sázava suite are metaluminous (A/CNK <1; Sázava intrusion and associated mafic rocks), whereas the Požáry trondhjemite falls within the peraluminous domain (A/CNK >1). In the Blatná suite, the Kozárovice granodiorite and monzonitic rocks are generally metaluminous, whereas the rest of the suite tends to be peraluminous. The more mafic members of the Čertovo břemeno suite are mainly metaluminous (Čertovo břemeno and Tábor intrusions) but the Sedlčany granite straddles the boundary of the peraluminous domain. The Říčany suite is almost exclusively peraluminous.

Trace elements

The granitoids of the CBP show a progressive increase in K_2O and Rb and decrease in K/Rb from Sázava to the Blatná, Čertovo břemeno and Říčany suites (Fig. 4; Table 1). The Sázava and Blatná suites have also lower Cs concentrations than both the Čertovo břemeno and Říčany suites.

Compared with the other suites within the CBP, the granitoids of the Sázava suite have low contents of high field strength elements (HFSE), except for Y (Fig. 4a). Such depletions are considered to be typical of subduction settings (e.g. Pearce *et al.*, 1984; Saunders *et al.*, 1991). This suite, including its more basic members, also has low contents of transition metals, particularly Cr and Ni, probably as a result of extensive fractionation. Chondrite-normalized rare earth element (REE) patterns for the majority of the suite are slightly light REE (LREE) enriched with Ce_N/Yb_N = 4·5–7·2, whereas those of the Požáry trondhjemites are U-shaped (Fig. 5a). The trondhjemites have total REE contents about half of those in the Sázava intrusion with a significantly higher LREE/HREE (heavy REE) ratio. The magnitude of the Eu anomaly is extremely variable, ranging from negative (Eu/Eu* = 0·7; Sázava tonalite) to positive (up to Eu/Eu* = 3·2; Požáry trondhjemite).

The Blatná suite has higher HFSE concentrations, although there is some overlap with the Sázava suite (Fig. 4b). The concentrations of Cr, Ni and Co are generally comparable, but somewhat higher in some of the monzonitic rocks. The REE patterns are steeper (Ce_N/Yb_N = 7·2–23·2) with moderate negative Eu anomalies (Eu/Eu* = 0·9–0·5) (Fig. 5b, c), except for monzonite Gbl-1 (Table 1).

The Čertovo břemeno suite has the highest HFSE concentrations, particularly of Zr, but Y is similar to the Sázava and Blatná suites (Fig. 4c). The suite typically has high contents of Cr and Ni, whereas Co is somewhat lower than in the Sázava suite (Table 1). The Čertovo břemeno suite is characterized by the highest ΣREE accompanied by high LREE/HREE ratios (Ce_N/Yb_N = 12·7–16·0) (Fig. 5d, e). All samples have negative Eu anomalies (Eu/Eu* = 0·6–0·9), with patterns of the mafic Čertovo břemeno intrusion and a minette nearly identical (Fig. 5d). The Tábor biotitite studied by Bowes & Košler (1993) is unusual in having a very pronounced negative Eu anomaly (Eu/Eu* = 0·3) and high ΣREE (Fig. 5e).

The trace-element geochemistry of the Říčany suite has been discussed by Janoušek *et al.* (1997*c*). In summary, the HFSE content in the Říčany granite is generally transitional between that of the Blatná and Čertovo břemeno suites although its Y is significantly lower (Fig. 4d). This suite is poor in all transition metals. The ΣREE is low and chondrite-normalized patterns are characterized by a strong LREE/HREE enrichment (Ce_N/Yb_N = 15–20) (Fig. 5f). The Říčany granite has a variable negative Eu anomaly and low contents of HREE. A sample of the late-stage leucogranite has low ΣREE = 55 and a slight positive Eu anomaly (Eu/Eu* = 1·2).

Sr–Nd isotope geochemistry

On the basis of the whole-rock Sr–Nd isotope geochemistry given by Janoušek *et al.* (1995), the earlier intrusions (Sázava suite) have Sr–Nd isotopic compositions close to Bulk Earth at 350 Ma, whereas the later intrusions shift towards more radiogenic Sr and less radiogenic Nd signatures (Říčany and Čertovo břemeno suites) (Fig. 6; Table 2). Overall, the isotopic data show a broad negative correlation with the total range of $(^{87}Sr/^{86}Sr)_{350}$ = 0·7050–0·7120 and ε_{Nd}^{350} = +0·4 to −8·7

Table 1: Selected whole-rock major- and trace-element data from the Central Bohemian Pluton

	Sázava suite								Blatná suite									
Intrusion:	Sázava				Teletín qtzd	gbd	Požáry		Kozárovice						monzonitic rocks			
Sample:	Sa-1	Sa-4	Sa-7	Sa-11	SaD-1	Gbs-2	Po-1	Po-4	Koz-2	Koz-4	Koz-5	Koz-6	Koz-9	Koz-12	KozD-1	Zal-1	Gbl-1	Gbl-2
Locality:	1	1	2	3	4	5	6	7	8	9	9	10	11	12	13	14	15	16
SiO_2	59·98	50·72	57·73	63·72	*52·90*	48·84	62·95	71·09	62·92	*64·79*	65·53	*62·59*	57·69	64·60	59·58	54·22	49·21	*49·62*
TiO_2	0·63	0·83	0·95	0·53	*1·35*	0·34	0·28	0·30	0·61	*0·52*	0·45	*0·67*	0·79	0·57	0·72	0·96	1·02	*0·60*
Al_2O_3	16·42	17·57	18·82	15·63	*18·23*	21·64	20·02	15·09	15·69	*15·28*	15·43	*15·66*	15·81	14·99	14·80	15·24	13·69	*9·06*
Fe_2O_3	1·35	2·19	1·00	1·31	*1·47*	3·28	0·67	0·38	0·86	*0·96*	1·46	*1·08*	2·11	1·27	1·69	1·17	2·47	*1·64*
FeO	5·46	7·65	5·43	4·44	*7·24*	2·74	1·65	2·12	3·51	*2·95*	2·34	*3·91*	4·07	2·79	4·08	6·12	6·96	*6·49*
MnO	0·19	0·24	0·12	0·14	*0·16*	0·13	0·05	0·06	0·10	*0·08*	0·09	*0·09*	0·13	0·08	0·14	0·15	0·15	*0·15*
MgO	3·21	5·18	2·82	2·13	*3·89*	5·11	0·55	0·52	2·96	*2·33*	2·14	*2·72*	4·70	2·37	4·11	4·94	8·53	*15·07*
CaO	7·04	9·92	7·47	5·24	*8·55*	13·75	6·61	3·75	4·65	*4·10*	3·76	*4·54*	5·39	3·44	5·33	7·17	9·74	*8·83*
Na_2O	2·52	2·83	2·54	3·38	*2·76*	1·78	3·91	3·68	3·30	*3·07*	3·25	*2·97*	3·15	3·12	2·84	2·44	1·89	*1·02*
K_2O	2·50	1·60	1·67	1·75	*1·45*	0·83	1·99	1·87	4·01	*3·95*	4·14	*3·77*	3·99	4·34	4·19	4·70	3·61	*3·27*
P_2O_5	0·16	0·19	0·37	0·12	*0·26*	0·04	0·07	0·07	0·26	*0·24*	0·21	*0·24*	0·26	0·21	0·37	0·80	0·76	*0·38*
H_2O^+	1·18	1·17	1·14	0·87	*1·53*	1·57	0·71	0·71	0·88	*0·80*	0·72	*0·97*	1·02	0·97	1·34	1·48	2·05	*2·55*
CO_2	0·18	0·09	0·13	0·34	*0·06*	0·51	0·35	0·27	0·13	*0·03*	0·06	*0·05*	0·26	0·21	0·19	0·05	0·16	*0·11*
Total	100·82	100·18	100·19	99·60	*99·85*	100·56	99·81	99·91	99·88	*99·10*	99·58	*99·26*	99·37	98·96	99·38	99·44	100·24	*98·79*
Mg/(Fe+Mg)	0·46	0·49	0·44	0·40	0·45	0·62	0·30	0·27	0·55	0·52	0·51	0·50	0·58	0·52	0·57	0·55	0·62	0·77
K/Rb	273·1	237·2	243·2	227·0	279·9	222·3	323·9	267·6	232·8	204·9	197·5	230·1	188·2	208·3	186·0	176·5	194·6	158·7
A/CNK	0·84	0·72	0·96	0·92	0·84	0·75	0·97	1·01	0·86	0·91	0·93	0·91	0·82	0·93	0·78	0·69	0·55	0·43
Ba	1037	388	722	1476	1017	245	1024	1284	1492	1135	1286	1289	1681	1154	1175	2224	2329	1351
Rb	76	56	57	64	43	31	51	58	143	160	174	136	176	173	187	221	154	171
Sr	539	472	537	378	430	278	599	430	500	430	418	409	519	385	379	510	540	218
Zr	76	56	57	74	88	27	128	180	216	201	201	218	251	211	146	251	62	77
Nb	6	5	10	5	10	8	5	6	—	—	14	13	16	11	9	16	11	7
Ga	17	19	20	16	18	14	18	14	18	18	17	20	17	16	20	19	18	14
Cr	29	53	33	50	43	159	15	16	84	99	113	76	147	57	171	198	496	1283
Ni	10	b.d.	b.d.	b.d.	b.d.	13	b.d.	b.d.	18	20	19	18	28	17	66	17	71	233
Co	17	30	13	13	18	23	b.d.	4	9	10	13	12	13	12	20	25	37	57
Pb	22	15	13	15	b.d.	13	21	29	34	37	46	29	31	36	42	31	19	12
Zn	71	104	50	73	85	51	23	22	52	50	49	60	69	52	85	85	85	59

	Sázava suite								Blatná suite									
Intrusion:	Sázava				Teletín qtzd	gbd	Požáry		Kozárovice						monzonitic rocks			
Sample:	Sa-1	Sa-4	Sa-7	Sa-11	SaD-1	Gbs-2	Po-1	Po-4	Koz-2	Koz-4	Koz-5	Koz-6	Koz-9	Koz-12	KozD-1	Zal-1	Gbl-1	Gbl-2
Locality:	1	1	2	3	4	5	6	7	8	9	9	10	11	12	13	14	15	16
La	—	21·7	20·8	—	20·0	—	11·6	26·2	35·0	—	—	34·8	—	32·7	25·9	43·9	27·7	26·0
Ce	—	71·8	42·0	—	46·8	—	18·0	39·0	64·4	—	—	68·3	—	58·4	58·3	94·3	60·3	54·1
Pr	—	6·9	5·0	—	6·1	—	1·8	3·9	7·9	—	—	8·2	—	7·3	7·8	11·7	7·7	7·1
Nd	—	29·7	17·4	—	23·5	—	5·4	11·5	27·5	—	—	29·4	—	24·9	28·6	45·5	29·2	26·0
Sm	—	6·2	3·8	—	5·9	—	1·4	1·8	5·7	—	—	6·0	—	4·9	5·9	10·0	7·0	6·4
Eu	—	1·5	1·8	—	2·0	—	1·3	1·0	1·5	—	—	1·6	—	1·3	1·5	2·5	2·2	1·6
Gd	—	6·1	3·8	—	6·2	—	1·1	1·4	4·7	—	—	5·3	—	4·3	4·9	8·4	7·0	5·8
Tb	—	0·9	0·6	—	1·0	—	0·1	0·2	0·7	—	—	0·8	—	0·6	0·7	1·0	0·7	0·8
Dy	—	5·8	2·7	—	5·1	—	0·6	0·8	3·5	—	—	4·1	—	3·1	3·4	5·6	3·7	4·2
Ho	—	1·0	0·6	—	1·1	—	0·1	0·1	0·6	—	—	0·7	—	0·6	0·6	1·0	0·7	0·8
Er	—	2·8	1·6	—	2·8	—	0·4	0·5	1·8	—	—	2·1	—	1·7	1·8	2·8	1·8	2·2
Tm	—	0·4	0·2	—	0·5	—	0·1	0·1	0·3	—	—	0·3	—	0·2	0·3	0·4	0·2	0·3
Yb	—	2·9	1·5	—	2·7	—	0·5	0·6	1·7	—	—	2·0	—	1·6	1·8	2·5	1·6	2·0
Lu	—	0·4	0·2	—	0·5	—	0·1	0·1	0·3	—	—	0·3	—	0·3	0·3	0·4	0·2	0·3
ΣREE	—	158·2	101·9	—	124·3	—	42·4	87·1	155·6	—	—	164·0	—	141·8	141·8	230·0	150·3	137·5
Eu/Eu*	—	0·7	1·4	—	1·0	—	3·2	2·1	0·9	—	—	0·8	—	0·8	0·8	0·8	1·0	0·8
Ce_N/Yb_N	—	6·4	7·2	—	4·5	—	9·2	16·6	9·6	—	—	8·9	—	9·4	8·2	9·6	9·9	7·1
Cs	—	5·7	6·6	—	2·3	—	3·0	3·0	9·9	—	—	6·8	—	13·0	21·3	17·7	7·8	13·1
Ta	—	0·5	0·6	—	1·1	—	0·3	0·2	1·2	—	—	0·7	—	1·1	1·5	1·1	0·7	0·8
Hf	—	2·5	3·6	—	1·8	—	4·2	5·4	5·8	—	—	6·1	—	7·2	4·7	13·3	4·3	5·0

Table 1: continued

	Blatná suite							Čertovo břemeno suite										Říčany s.
Intrusion:	Blatná							Sedlčany						Čert. bř.	Tábor	minettes		Říčany
Sample:	Bl-1	Bl-2	Bl-4	Bl-7	Bl-8	Cv-1	Cv-3	Se-1	Se-5	Se-6	Se-9	Se-12	Se-15	Cb-3	Ta-1	Mi-1	Mi-2	Ri-1
Locality:	17	18	19	20	21	22	23	24	25	25	24	26	27	28	29	30	31	32
SiO_2	67·08	*63·16*	68·11	67·80	62·94	62·88	61·86	*66·58*	65·87	66·70	67·74	69·06	66·47	55·96	*59·69*	58·32	*56·22*	71·43
TiO_2	0·50	*0·79*	0·52	0·49	0·70	0·76	0·73	*0·60*	0·63	0·56	0·54	0·53	0·60	1·07	*0·91*	0·88	*1·45*	0·30
Al_2O_3	14·88	*16·33*	15·43	15·43	15·74	16·15	16·17	*14·58*	14·41	14·72	14·55	14·37	14·47	13·62	*14·13*	12·27	*12·47*	14·58
Fe_2O_3	0·81	*0·50*	0·68	0·55	0·60	0·88	0·81	*0·51*	0·56	0·54	0·57	0·29	0·52	2·29	*0·38*	1·69	*1·51*	0·26
FeO	2·43	*3·82*	2·19	2·24	3·92	3·90	4·18	*2·55*	2·53	2·33	2·53	2·43	2·66	3·56	*4·51*	4·11	*3·97*	0·99
MnO	0·06	*0·07*	0·05	0·05	0·11	0·07	0·10	*0·06*	0·06	0·07	0·07	0·03	0·06	0·13	*0·08*	0·10	*0·09*	0·01
MgO	1·82	*2·64*	1·61	1·59	3·17	3·49	3·58	*2·53*	2·53	2·56	2·38	2·19	2·55	7·33	*5·07*	8·25	*7·97*	1·12
CaO	2·76	*3·62*	2·82	2·70	4·31	4·44	3·98	*2·36*	2·37	2·35	2·24	2·06	2·39	4·11	*3·72*	3·60	*3·83*	1·27
Na_2O	3·64	*3·36*	3·45	3·40	3·08	2·62	2·94	*2·69*	2·63	2·70	2·32	2·53	2·68	2·16	*2·07*	1·83	*1·34*	3·32
K_2O	4·07	*3·57*	4·12	4·38	3·55	3·67	3·56	*5·80*	5·85	5·69	5·54	5·36	5·62	6·67	*6·82*	6·12	*7·20*	5·29
P_2O_5	0·17	*0·29*	0·17	0·17	0·24	0·28	0·26	*0·36*	0·38	0·33	0·33	0·29	0·36	0·89	*0·67*	0·66	*0·89*	0·17
H_2O^+	1·00	*0·97*	0·79	0·63	1·13	1·01	1·01	*0·90*	0·92	0·76	0·77	0·68	0·88	1·53	*0·80*	1·50	*2·09*	0·51
CO_2	0·37	*0·06*	0·06	0·04	0·27	0·14	0·19	*0·04*	0·03	0·25	0·26	0·33	0·04	0·19	*0·04*	0·51	*0·25*	0·03
Total	99·59	99·18	100·00	99·47	99·76	100·29	99·37	99·56	98·77	99·56	99·84	100·15	99·30	99·51	98·89	99·84	99·28	99·28
Mg/(Fe + Mg)	0·51	0·52	0·51	0·51	0·56	0·57	0·57	0·60	0·60	0·62	0·58	0·59	0·59	0·70	0·65	0·72	0·73	0·62
K/Rb	169·8	160·2	180·0	207·8	200·5	230·8	173·8	166·0	156·1	155·4	147·9	151·9	131·8	153·8	159·5	124·2	170·8	137·2
A/CNK	0·97	1·02	1·01	1·01	0·94	0·99	1·02	0·97	0·96	0·99	1·05	1·05	0·98	0·75	0·81	0·76	0·74	1·08
Ba	963	1204	900	928	1080	1149	1181	1079	1126	1115	1076	1002	1084	2109	1797	1578	2084	901
Rb	199	185	190	175	147	132	170	290	311	304	311	293	354	360	355	409	350	320
Sr	333	413	348	338	361	412	368	318	354	358	312	312	302	495	418	355	350	378
Zr	177	188	171	149	169	226	146	237	283	269	256	259	229	405	390	372	544	240
Nb	12	12	13	18	14	9	14	14	16	17	20	16	19	23	13	20	—	21
Ga	21	23	19	20	b.d.	23	22	20	20	20	19	18	19	20	19	18	18	24
Cr	61	111	50	54	114	75	131	168	160	132	166	122	157	498	425	504	486	43
Ni	18	25	15	16	31	24	38	33	24	26	30	27	45	135	59	235	127	11
Co	8	11	10	7	12	15	16	10	12	12	8	5	12	28	22	28	30	b.d.
Pb	40	24	41	43	24	17	34	53	70	68	68	63	60	34	46	53	69	66
Zn	63	79	58	54	51	74	84	55	58	50	53	52	62	85	76	79	70	34

	Blatná suite							Čertovo břemeno suite										Říčany s.
Intrusion:	Blatná							Sedlčany						Čert. bř.	Tábor	minettes		Říčany
Sample:	Bl-1	Bl-2	Bl-4	Bl-7	Bl-8	Cv-1	Cv-3	Se-1	Se-5	Se-6	Se-9	Se-12	Se-15	Cb-3	Ta-1	Mi-1	Mi-2	Ri-1
Locality:	17	18	19	20	21	22	23	24	25	25	24	26	27	28	29	30	31	32
La	—	55·2	39·8	33·1	42·9	45·6	—	109·3	43·9	—	44·2	—	44·5	44·8	54·0	52·6	—	18·2
Ce	—	111·1	80·9	66·2	94·6	99·6	—	—	91·8	—	92·3	—	96·8	110·2	125·3	119·1	—	35·4
Pr	—	12·7	9·6	8·0	11·9	12·4	—	20·6	11·5	—	11·7	—	11·5	15·5	17·0	15·8	—	4·2
Nd	—	42·5	31·6	26·7	43·3	44·9	—	63·0	40·8	—	42·1	—	39·9	61·7	62·8	58·8	—	15·2
Sm	—	7·2	5·6	5·5	9·4	9·8	—	10·4	8·4	—	8·8	—	8·3	14·6	13·7	13·8	—	2·9
Eu	—	1·7	1·2	1·2	1·9	1·7	—	2·1	1·7	—	1·8	—	1·7	3·5	2·9	3·4	—	0·7
Gd	—	5·9	4·7	4·7	8·2	9·2	—	12·4	6·2	—	6·4	—	6·6	10·7	10·7	10·0	—	2·1
Tb	—	0·7	0·6	0·7	1·2	1·2	—	1·1	0·8	—	0·9	—	0·8	1·2	1·2	1·1	—	0·3
Dy	—	3·4	3·1	3·4	5·8	6·6	—	4·5	3·9	—	4·1	—	4·0	5·8	5·9	5·1	—	1·3
Ho	—	0·5	0·5	0·6	1·1	1·2	—	0·7	0·7	—	0·7	—	0·6	0·9	1·0	0·8	—	0·2
Er	—	1·4	1·6	1·8	2·9	3·2	—	2·0	1·9	—	2·0	—	1·7	2·5	2·6	2·3	—	0·6
Tm	—	0·2	0·3	0·3	0·5	0·4	—	0·3	0·3	—	0·3	—	0·2	0·3	0·3	0·3	—	0·1
Yb	—	1·2	1·8	1·8	2·7	2·6	—	1·9	1·7	—	1·9	—	1·6	2·1	2·1	1·9	—	0·6
Lu	—	0·2	0·3	0·3	0·4	0·3	—	0·3	0·3	—	0·3	—	0·2	0·3	0·3	0·3	—	0·1
ΣREE	—	244·0	181·7	154·0	226·7	238·5	—	—	213·9	—	217·4	—	218·6	274·2	299·9	285·3	—	81·9
Eu/Eu*	—	0·8	0·7	0·7	0·7	0·5	—	0·6	0·7	—	0·7	—	0·7	0·8	0·7	0·9	—	0·9
Ce_N/Yb_N	—	23·2	11·5	9·8	9·2	10·1	—	—	13·7	—	12·7	—	15·7	13·6	15·5	16·0	—	15·0
Cs	—	12·2	18·8	17·4	8·5	6·4	—	30·0	51·6	—	31·7	—	48·9	27·0	23·7	55·5	—	66·0
Ta	—	1·4	1·4	1·7	1·5	1·0	—	2·4	2·9	—	2·4	—	4·4	1·8	1·7	2·2	—	2·3
Hf	—	3·8	6·3	9·9	4·5	3·3	—	6·7	8·5	—	9·1	—	6·7	12·8	4·3	10·8	—	8·8

The XRF analyses (most major elements, all trace elements Ba–Zn) were carried out using a Philips PW 1450/20 automatic sequential XRF spectrometer at the University of Glasgow. Ferrous iron was determined by potassium dichromate titration with 0·2% solution of sodium diphenylamine sulphonate as an indicator (Pratt, 1894) following a combined H_2SO_4–HNO_3–HF acid attack. The REE were analysed using a VG Plasma Quad PQ1, and Cs, Ta and Hf using a VG Plasma Quad PQ2 Turbo Plus ICP-MS; analyses were carried out at SURRC, East Kilbride, UK. Full analytical details and precise sample location have been given by Janoušek (1994). Major-element analyses shown in italics were carried out using standard methods of wet chemistry in the laboratories of the Czech Geological Survey, Prague.

Sázava suite

Sázava intrusion: 1, biotite–amphibole quartz diorite, Mrač, quarry; 2, biotite–amphibole tonalite, Teletín, disused quarry; 3, biotite–amphibole quartz diorite, Prosečnice, quarry. Basic rocks: 4, biotite–amphibole quartz diorite, Teletín, disused quarry; 5, amphibole–biotite quartz gabbrodiorite, Vavřetice. Požáry intrusion: 6, biotite trondhjemite, Krhanice, quarry; 7, biotite trondhjemite, Prosečnice, quarry.

Blatná suite

Kozárovice intrusion: 8, biotite–amphibole granodiorite, Kozárovice, quarry; 9, amphibole–biotite granodiorite, Kozárovice, quarry; 10, porphyritic amphibole–biotite granodiorite, Kozárovice, disused quarry; 11, biotite–amphibole granodiorite, Hříměždice, disused quarry; 12, porphyritic amphibole–biotite granodiorite ('Těchnice type'), Kamýk nad Vltavou, rock outcrop. Monzonitic rocks: 13, biotite–amphibole quartz monzonite, Kozárovice, quarry; 14, pyroxene–biotite–amphibole quartz monzonite, Zalužany, disused quarry; 15, pyroxene–biotite–amphibole monzonite, Lučkovice, disused quarry; 16, (pyroxene–) biotite–amphibole monzonite, Lučkovice, disused quarry. Blatná intrusion: 17, (amphibole–) biotite granodiorite, Řečice, quarry; 18, (amphibole–) biotite granodiorite, Tužice, quarry; 19, biotite granodiorite, Paštiky, disused quarry; 20, biotite granodiorite, Defurovy Lažany, quarry; 21, amphibole–biotite granodiorite, Hudčice, quarry; 22, amphibole–biotite granodiorite ('Červená type'), Vlčkovice, quarry; 23, amphibole–biotite granodiorite ('Červená type'), Horaždťovice, quarry.

Čertovo břemeno suite

Sedlčany intrusion: 24, (amphibole–) biotite granite, Vrchotovy Janovice, quarry; 25, amphibole–biotite granite, Vápenice, quarry; 26, biotite granite, Kosova Hora, quarry; 27, amphibole–biotite granite, Vrchotovy Janovice, quarry. Čertovo břemeno intrusion: 28, porphyritic biotite–amphibole syenite, Chyšky, well at water tower (elevation 685 m). Tábor intrusion: 29, pyroxene–biotite quartz syenite, Tábor-Klokoty, disused quarry; 30, minette, Kožlí, quarry; 31, minette, Zalužany, disused quarry.

Říčany suite

Říčany intrusion: 32, porphyritic (muscovite)–biotite granite, Žernovka, quarry. Additional analyses for the Říčany suite were given elsewhere (Janoušek *et al.*, 1997*c*).

qtzd, quartz diorite; gbd, gabbrodiorite.

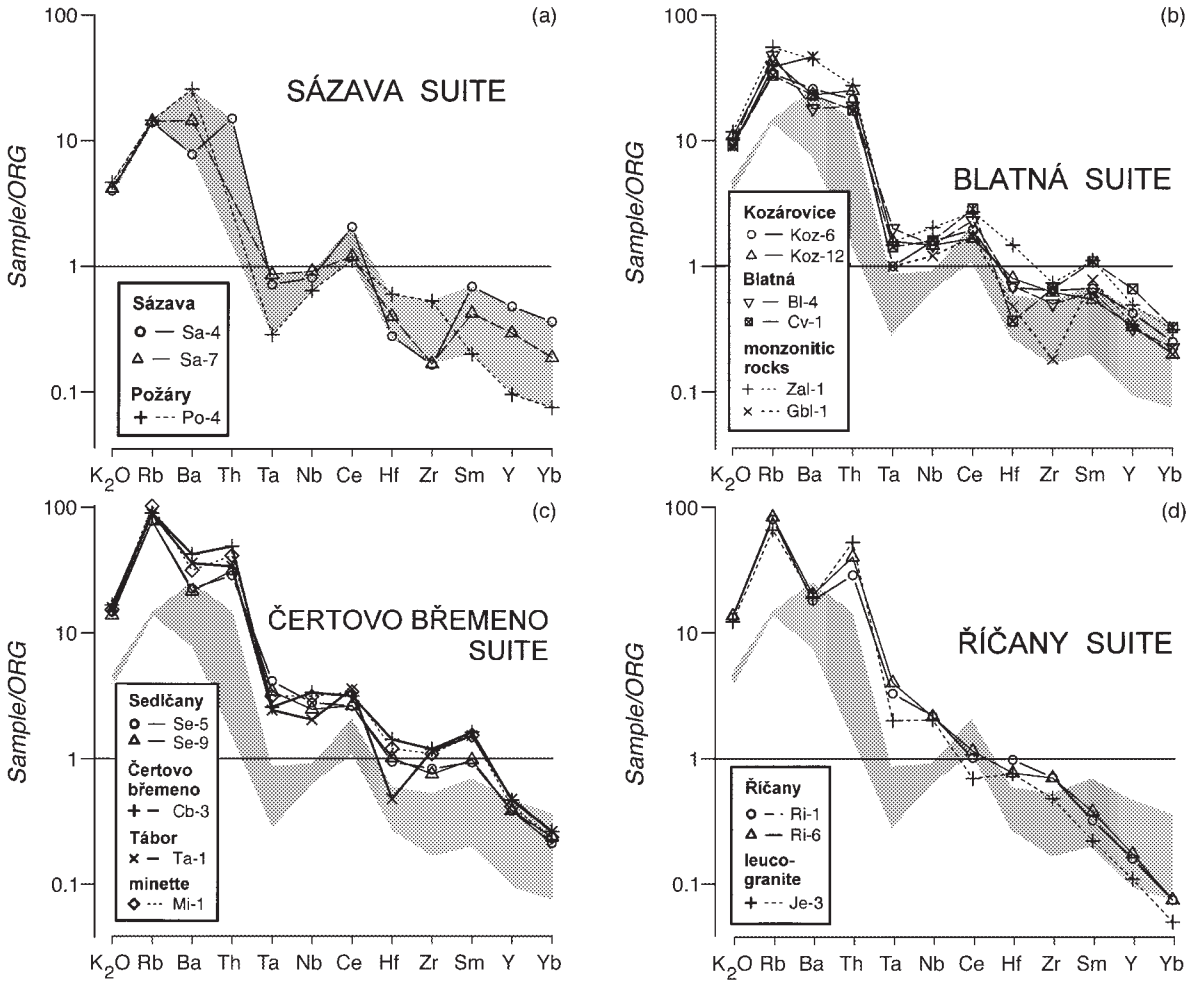

Fig. 4. Ocean ridge granite (ORG) normalized multi-element diagrams for selected analyses from the four main suites of the Central Bohemian Pluton; normalizing values from Pearce *et al.* (1984); shaded field of the Sázava suite (a) shown on all plots for comparison.

(Table 2). As demonstrated by Janoušek *et al.* (1995, 1997*b*) and below, this cannot be interpreted as a simple contamination trend, but it reflects major differences in sources and processes involved in genesis of particular granitoid suites and intrusions.

GEOCHEMICAL MODELLING

The causes of the geochemical variation within each suite were investigated using major- and trace-element modelling. In the case of the fractional crystallization, major-element modelling was based on the general least-squares mixing equation of Bryan *et al.* (1969) and was performed using the IgPet package. Those oxides that were not determined or that had very low concentrations in all the studied minerals and rocks (MnO and P_2O_5) were omitted; total iron content (FeO^T) was used instead of the separate FeO and Fe_2O_3. Typical mineral analyses for each particular intrusion were used (Janoušek, 1994); the choice of whole-rock end-members was based on Harker plots and the R_1–R_2 plot (Fig. 7: De la Roche *et al.*, 1980; Batchelor & Bowden, 1985). The quality of the model was assessed by the sum of squares of the residuals (R^2), with $R^2 = 0$ for the ideal fit; $R^2 < 1$ was considered to be acceptable. This approach was repeated for several parent–daughter combinations to check the robustness of the modelling; the ranges of obtained solutions are given below and representative examples are given in Table 3. The major-element, Rb–Sr–Ba and, if applicable, REE data were then modelled using the fractionation schemes derived from the major elements (see Table 4 for distribution coefficients).

Whenever a magma-mixing scenario was invoked, it was quantified by a mixing test using major elements (Fourcade & Allègre, 1981). Its principle is that all the

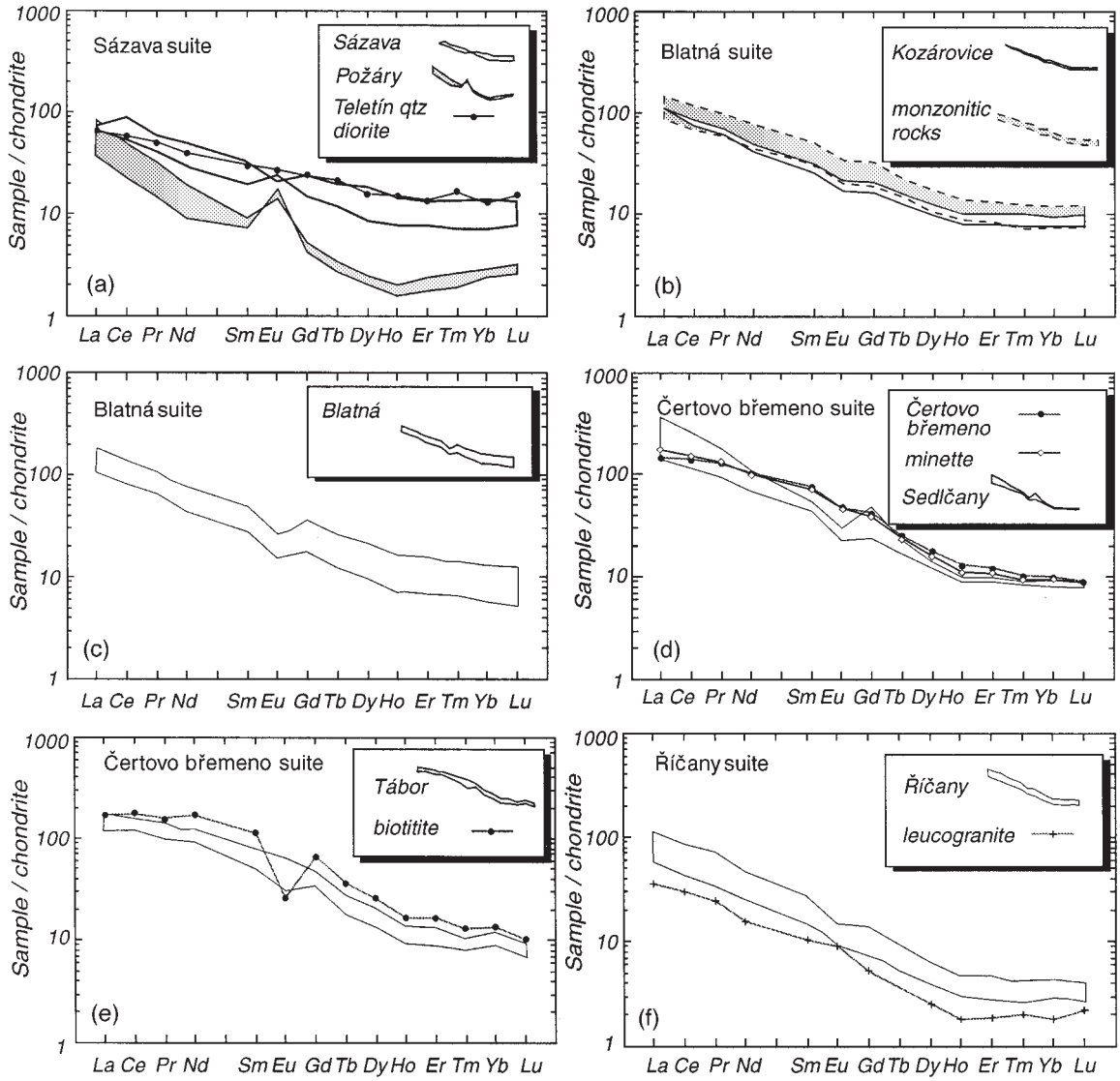

Fig. 5. Chondrite-normalized REE patterns for the Central Bohemian Pluton granitoid suites and intrusions; data from Table 1 and Bowes & Košler (1993); composition of the CI chondrite used for normalization from Boynton (1984).

oxides of a sample that originated by magma mixing should plot on a straight line in a diagram of $c_a - c_b$ vs $c_h - c_b$ (where c_a, c_b and c_h stand for wt % oxide in the acid end-member, basic end-member, and suspected hybrid, respectively) with the slope being equivalent to the proportion of the component *a*. The results were then tested on the trace-element data by comparison of the calculated and observed contents of the putative hybrids (Castro *et al.*, 1990).

Sázava suite

The geochemical characteristics of the Sázava suite (mainly metaluminous, $K_2O \ll Na_2O$; $(^{87}Sr/^{86}Sr)_{350} \sim 0{\cdot}705$, $\varepsilon_{Nd}^{350} \sim 0$ for the Sázava tonalite; Fig. 6) correspond to those of a typical I-type granitoid (e.g. Clarke, 1992, and references therein). The Harker plots (Fig. 8) show a negative correlation of SiO_2 with CaO, MgO, TiO_2 and Y, and a positive correlation with K_2O, Rb and Ba. Such trends are consistent with fractionation

Table 2: Sr–Nd isotopic data for rocks of the Central Bohemian Pluton (Janoušek et al., *1995) age-corrected to 350 Ma*

	Sázava suite		Blatná suite								
Intrusion:	Sázava		Kozárovice					Blatná		monzonitic rocks	
	Sa-1	Sa-3	Koz-2	Koz-4	Koz-5	Koz-6	Koz-12	Bl-2	Cv-1	Gbl-1	Gbl-2
Rb (ppm)	76	55	164·1	174·5	181·9	146·7	172·9	185	132	138·2	171
Sr (ppm)	555·8	606·1	486·9	437·6	410·3	417·7	398·5	439·1	404·6	547·5	221·3
$^{87}Rb/^{86}Sr$	0·3955	0·2627	0·9767	1·1544	1·2838	1·0167	1·2564	1·2189	0·9438	0·7305	2·2389
$^{87}Sr/^{86}Sr$	0·70700(3)	0·70638(3)	0·71258(4)	0·71367(3)	0·71434(4)	0·71209(3)	0·71373(4)	0·71434(3)	0·71362(4)	0·71114(4)	0·71863(4)
$^{87}Sr/^{86}Sr_{350}$	0·70503	0·70507	0·70771	0·70792	0·70794	0·70703	0·70747	0·70827	0·70891	0·70750	0·70747
Sm (ppm)	4·57	6·66	5·91	5·36	5·04	6·23	—	6·85	10·83	6·39	6·09
Nd (ppm)	24·2	33·9	31·7	28·9	26·7	33·4	—	43·8	50·1	31·7	26·9
$^{147}Sm/^{144}Nd$	0·1188	0·1189	0·1128	0·1121	0·1141	0·1127	—	0·0946	0·1307	0·1217	0·1366
$^{143}Nd/^{144}Nd$	0·512476(6)	0·512479(7)	0·512210(7)	0·512186(5)	0·512187(7)	0·512267(7)	—	0·512101(7)	0·512225(6)	0·512316	0·512334(7)
$^{143}Nd/^{144}Nd_{350}$	0·512204	0·512207	0·511952	0·511929	0·511926	0·512009	—	0·511884	0·511925	0·512037	0·512021
ε_{Nd}^{350}	0·3	0·4	−4·6	−5·0	−5·1	−3·5	—	−5·9	−5·1	−2·9	−3·2

	Čertovo břemeno suite					Říčany suite					
Intrusion:	Sedlčany			minettes		Říčany					
	Se-1	Se-5	Se-9	Mi-2	Mi-1	Ri-1	Ri-2	Ri-4	Ri-5	Ri-6	Ri-10
Rb (ppm)	310·9	314·4	308·1	350	421·8	310·7	326·9	319·2	310·4	317·3	322·9
Sr (ppm)	313·9	339	307·8	333·7	354·1	374·1	360·2	377·7	399·5	386·6	322·4
$^{87}Rb/^{86}Sr$	2·8703	2·6879	2·9016	3·0408	3·4540	2·4058	2·6299	2·4483	2·2510	2·3776	2·9034
$^{87}Sr/^{86}Sr$	0·72615(3)	0·72543(3)	0·72620(3)	0·72700(4)	0·72907(4)	0·72154(3)	0·72267(3)	0·72216(4)	0·72134(4)	0·72186(3)	0·72431(3)
$^{87}Sr/^{86}Sr_{350}$	0·71185	0·71204	0·71174	0·71185	0·71187	0·70955	0·70956	0·70996	0·71013	0·71001	0·70984
Sm (ppm)	8·26	7·88	8·17	16·25	12·60	4·06	4·98	4·59	3·83	4·56	4·40
Nd (ppm)	40·0	40·2	40·2	75·9	61·7	24·1	29·0	27·9	23·6	28·1	26·5
$^{147}Sm/^{144}Nd$	0·1253	0·1186	0·1228	0·1293	0·1235	0·1020	0·1005	0·0995	0·0980	0·0980	0·1005
$^{143}Nd/^{144}Nd$	0·512114(7)	0·512103(8)	0·512080(10)	0·512140(7)	0·512113(7)	0·512053(6)	0·512035(6)	0·512062(11)	0·512074(14)	0·512068(7)	0·512075(9)
$^{143}Nd/^{144}Nd_{350}$	0·511827	0·511831	0·511799	0·511844	0·51183	0·511819	0·511805	0·511834	0·511849	0·511843	0·511845
ε_{Nd}^{350}	−7·0	−7·0	−7·6	−6·7	−7·0	−7·2	−7·5	−6·9	−6·6	−6·7	−6·7

Analytical details have been given by Janoušek *et al.* (1995); sample descriptions and locations are given in Table 1 and by Janoušek *et al.* (1995); errors in parentheses are 2 SE.

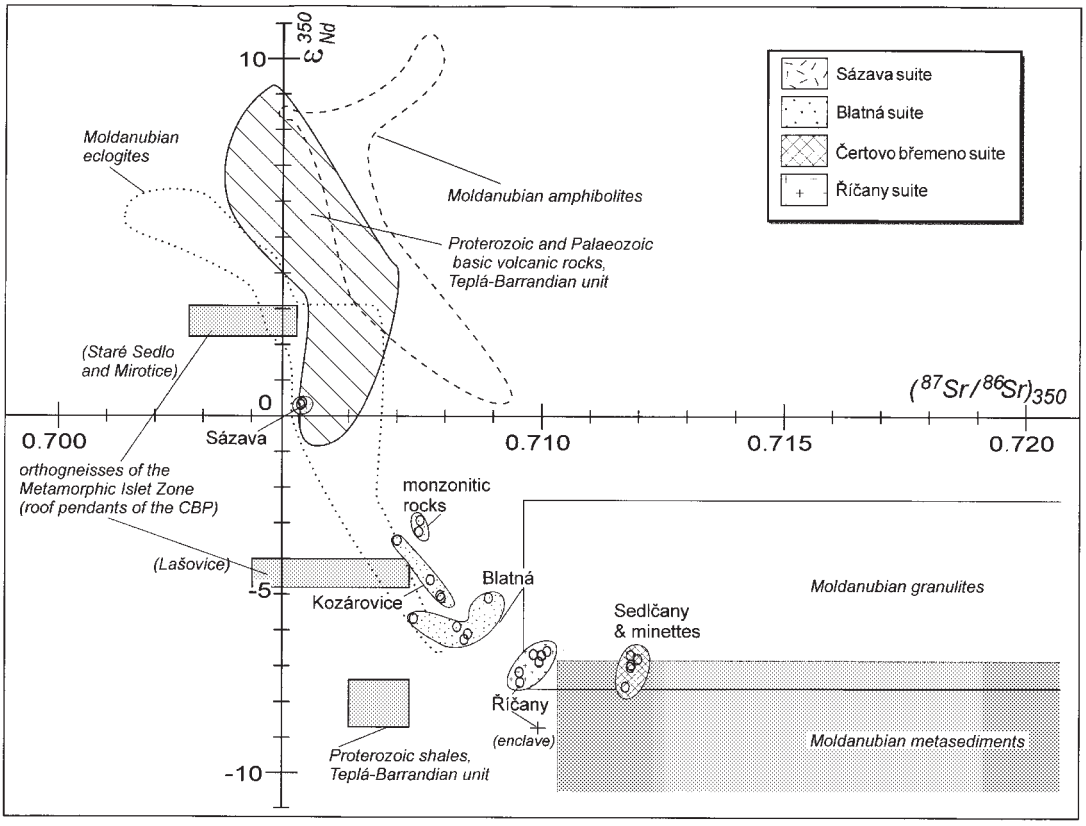

Fig. 6. $(^{87}Sr/^{86}Sr)_{350}$ vs ε_{Nd}^{350} plot for granitoids of the Central Bohemian Pluton [after Janoušek *et al.* (1995) and references therein]; distribution of the main geological units is shown in Fig. 1; fields of Moldanubian metasediments and granulites partly based on unpublished data.

dominated by amphibole and calcic plagioclase, as also revealed by the R_1–R_2 plot (Fig. 7). A major role for biotite and K-feldspar fractionation is unlikely in view of their interstitial habit (Janoušek, 1994). Least-squares modelling (e.g. Table 3) shows that the compositional spectrum of the Sázava intrusion can be explained by extensive (up to 82%) fractionation of ~52% amphibole, 43% plagioclase and 5% biotite. A high degree of fractionation (~65–75%) can be inferred independently from the concentrations of strongly incompatible elements such as Ba (Fig. 8d).

With the Sázava suite showing the least evolved major- and trace-element geochemistry, a primitive Sr–Nd isotopic signature (close to Bulk Earth), and an abundance of mafic microgranular enclaves (interpreted as hybrids of acidic and basic magmas; e.g. Didier & Barbarin, 1991, p. 23), a significant role for mantle-derived material in its genesis is indicated. On the basis of the Sr–Nd isotope data the suite could have formed by (1) crystallization from (asthenospheric?) mantle-derived melts with an isotopic composition close to Bulk Earth, (2) melting of local metabasic rocks that have a similar Sr–Nd signature, or (3) mixing of melts derived from both sources (Janoušek *et al.*, 1995). Although there exists considerable field, microstructural, mineral and whole-rock geochemical evidence for mixing and mingling between mafic and felsic magmas, at least in the western part of the Sázava intrusion (e.g. in Teletín: Dudek & Fediuk, 1957; Janoušek, 1994; Janoušek *et al.*, 1997*a*; see Fig. 7), derivation for the whole compositional range of the suite in this manner seems unlikely: the associated basic rocks do not form a continuum with the Sázava samples on the R_1–R_2 plot (Fig. 7), and do not have low enough SiO_2 contents (Janoušek, 1994).

Taking into account the near contemporaneity of both the Sázava and Požáry intrusions (Holub *et al.*, 1997*a*), the Požáry trondhjemites, characterized by low ΣREE and positive Eu anomalies, could, in theory, have been derived in three ways: (1) by plagioclase accumulation from a Sázava-like parent, (2) by fractional crystallization from a similar melt of a largely amphibole–plagioclase assemblage, or (3) by variable, but low degrees of partial melting of a metabasic source leaving amphibole ± garnet in the residue [to explain the observed low middle REE (MREE) and HREE contents].

Although plagioclase accumulation probably played an important role in the genesis of some of the Požáry samples (e.g. Po-1 in Fig. 8, a rock that shows a

Table 3: Examples of major-element based modelling of fractional crystallization using the least-squares model of Bryan et al. *(1969)*

	plg2 An_{54}*	bi3	amph7	Sa-4†	Sa-11†	Difference		Solution‡	Cumulate§
	Sa-3	Sa-3	Sa-3	recalc 100%	recalc 100%	(obs – calc)	Sa-4	1·000	%
Sázava intrusion									
SiO_2	53·41	35·32	45·35	51·61	65·02	0·00	plg	−0·345	42·8
TiO_2	0·00	2·11	1·39	0·84	0·54	0·06	bi	−0·043	5·3
Al_2O_3	29·48	15·31	9·47	17·88	15·95	−0·06	amph	−0·418	51·9
FeO^T	0·09	23·56	18·57	9·79	5·73	−0·24	Sa-11	0·189	R^2 = 0·314
MgO	0·00	9·05	9·82	5·27	2·17	0·30			
CaO	11·27	0·01	11·92	10·09	5·35	0·13			
Na_2O	5·05	0·10	1·08	2·88	3·45	0·01			
K_2O	0·12	9·81	1·02	1·63	1·79	0·38			
	plg10 An_{50}	KF1	bi4	amph5	Koz-9	Koz-12	Difference		Solution	Cumulate
	Koz-2	Koz-4	Koz4	Koz4	recalc 100%	recalc 100%	(obs – calc)	Koz-9	1·000	%
Kozárovice intrusion										
SiO_2	54·13	63·01	35·60	45·95	59·18	66·35	−0·02	plg	−0·139	32·4
TiO_2	0·04	0·00	3·80	1·04	0·81	0·59	0·05	KF	−0·053	12·3
Al_2O_3	29·96	19·35	14·66	7·55	16·22	15·40	0·03	bi	−0·056	13·0
FeO^T	0·06	0·09	19·47	16·10	6·12	4·04	−0·38	amph	−0·181	42·3
MgO	0·00	0·00	10·02	11·29	4·82	2·463	0·71	Koz-12	0·566	R^2 =0·798
CaO	10·49	0·04	0·03	11·79	5·53	3·53	−0·15			
Na_2O	5·53	1·05	0·12	1·29	3·23	3·20	0·35			
K_2O	0·11	14·93	9·39	0·86	4·09	4·46	0·03			
	amph1	plg $3An_{38}$	bi1	Cv-3	Bl-1	Difference		Solution	Cumulate	
	Bl-5	Bl-7	Bl-7	recalc 100%	recalc 100%	(obs – calc)	Cv-3	1·000	%	
Blatná intrusion										
SiO_2	45·75	57·49	36·04	63·30	68·51	0·02	amph	−0·081	26·2	
TiO_2	1·15	0·00	3·35	0·75	0·51	0·00	plg	−0·144	46·8	
Al_2O_3	7·02	26·69	14·59	16·55	15·20	0·17	bi	−0·083	26·9	
FeO^T	16·41	0·02	18·90	5·02	3·23	−0·29	Bl-1	0·699	R^2 = 0·813	
MgO	11·74	0·00	11·28	3·66	1·86	0·38				
CaO	11·89	8·04	0·03	4·07	2·82	−0·07				
Na_2O	1·16	7·02	0·11	3·01	3·72	−0·72				
K_2O	0·78	0·16	9·61	3·64	4·16	−0·20				

Table 3: continued

	bi1 Se-6	plg3An$_{42}$ Se-5	KF1 Se-5	amph4 Se-9	Se-6 recalc 100%	Se-12 recalc 100%	Difference (obs – calc)	Se-6	Solution 1·000	Cumulate %
Sedlčany intrusion										
SiO_2	36·85	56·61	62·99	50·82	67·95	69·88	0·00	bi	−0·016	11·9
TiO_2	2·95	0·02	0·02	0·36	0·57	0·54	−0·05	KF	−0·057	41·8
Al_2O_3	14·15	26·82	18·69	4·15	14·99	14·54	0·04	plg	−0·040	29·4
FeO^T	16·28	0·08	0·07	13·86	2·87	2·72	0·09	amph	−0·023	16·9
MgO	13·82	0·00	0·00	14·71	2·61	2·22	−0·11	Se-12	0·861	R^2 =0·071
CaO	0·00	8·63	0·05	11·22	2·39	2·08	0·02			
Na_2O	0·08	6·51	0·89	0·89	2·75	2·56	−0·21			
K_2O	10·03	0·22	15·35	0·37	5·80	5·42	−0·05			

FeO^T total iron as FeO.
*Mineral analyses (Janoušek, 1994).
†Original whole-rock analyses of presumed parent and daughter recalculated to 100%.
‡Proportion of particular minerals removed relative to the parent (=1); (1 − total) × 100 corresponds to degree of fractionation (here 81·1%).
§Percentage of particular minerals in the cumulate.

Table 4: Trace-element partition coefficients used for modelling

Mineral	La	Ce	Nd	Sm	Eu	Gd	Tb	Yb	Lu	Ref.	Y	Ref.	Rb	Sr	Ba	Ref.
amphibole	0·85	1·2	3·2	5·4	3·6	10 (1)	3	6·2	4·5	(2)	6	(3)	0·014	0·22	0·044	(4)
plagioclase	0·32	0·24	0·19	0·13	2·00	0·16	0·15	0·08	0·06	(2)	0·1	(3)	0·041	4·4	0·31	(4)
biotite	0·32	0·04	0·04	0·06	0·15	0·44	0·39	0·67	0·74	(2)	0·03	(3)	3·26	0·12	6·36	(4)
K-feldspar	0·072	0·046	0·038	0·025	2·6	0·011	0·033	0·02	0·03	(3)			0·659	3·87	6·12	(4)
allanite	1331	1279	874	438	107	214	204	22	22	(5)						
titanite	60	90	103	340	157	383	326	231	176	(5)						
zircon	3·3	2·4	2·2	3·7	3·4	13·9	26·3	225	300	(5)						
apatite	46·1	41·6	55·8	65	27·3	79	60	60	60	(5)						

References: (1) Martin (1987); (2) Henderson (1982); (3) Rollinson (1993) and references therein; (4) Hanson (1978); (5) Sawka (1988).

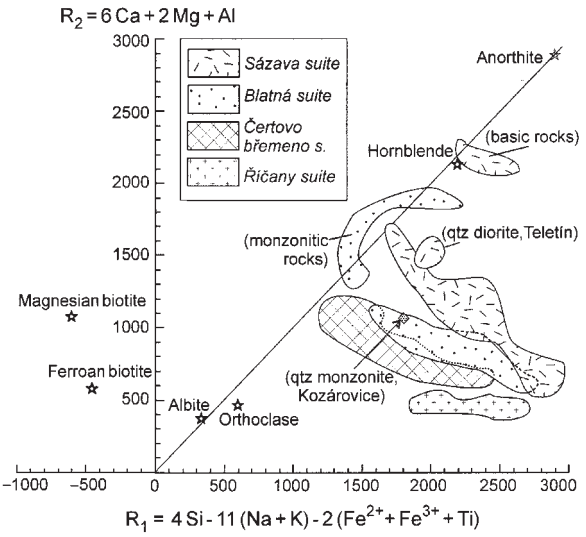

Fig. 7. Fields of the four main suites of the Central Bohemian Pluton on a plot of the multicationic R_1 and R_2 parameters of De la Roche *et al.* (1980); the compositions of common granitoid rock-forming minerals also plotted [after Batchelor & Bowden (1985)].

cumulate-like texture), a purely cumulative origin from the Sázava magma is ruled out because this would require the Sázava melt to be driven towards less silicic compositions. Moreover, such a model would necessitate early crystallization of a plagioclase–quartz assemblage (as the trondhjemites are more silica rich than their feldspars) without a significant proportion of amphibole. This, together with amphibole being only an accessory phase in the trondhjemite, is not in accord with the evidence of early simultaneous crystallization of plagioclase and amphibole in the Sázava intrusion.

The observed progressive decrease in REE and Y contents suggests a major role for either amphibole or some accessory mineral(s) (e.g. titanite, allanite)—the only phases that have distribution coefficients for these elements generally >1. This is consistent with the evidence for amphibole-dominated fractionation inferred from major elements. By 30–50% fractionation of the assemblage for the Sázava intrusion in Table 3 (calculated by the least-squares method), it is possible to generate HREE patterns similar to the trondhjemite from the least

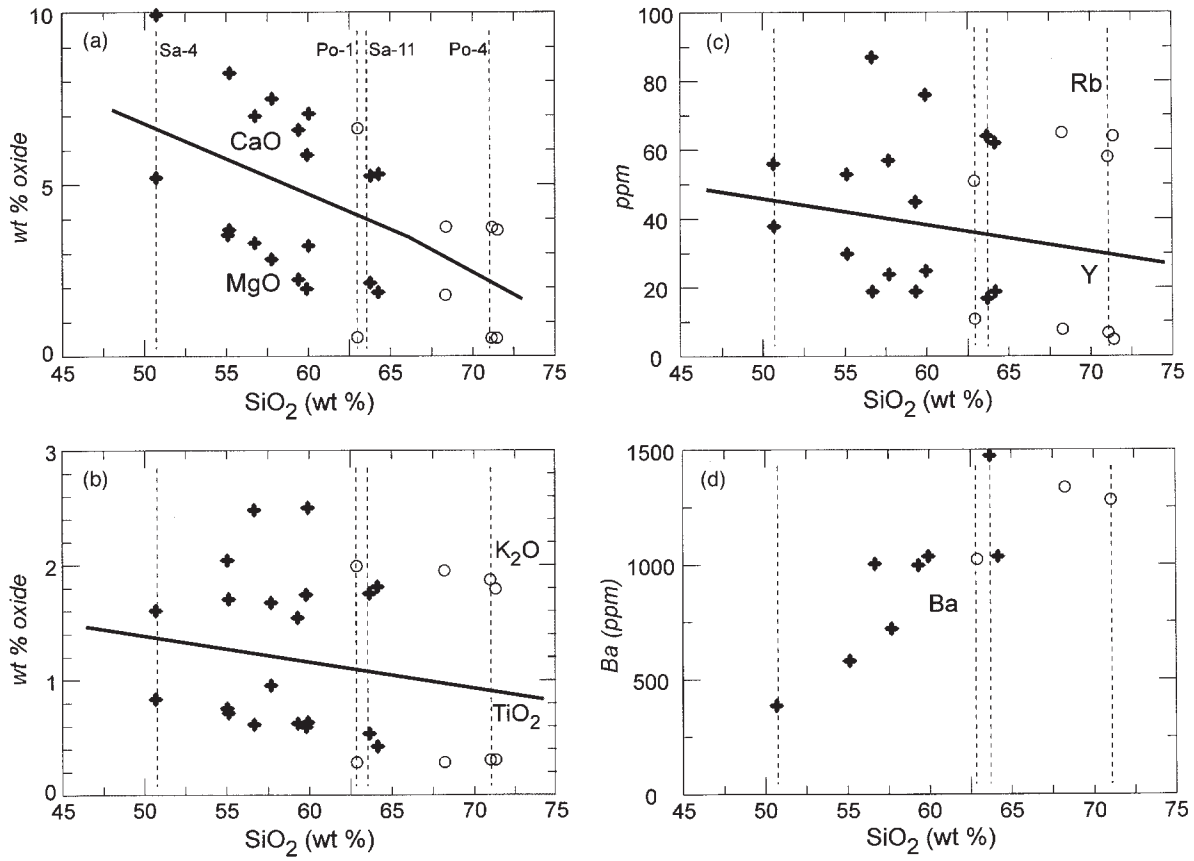

Fig. 8. Variation of silica vs selected major- and trace-element compositions for whole-rock samples from the Sázava (filled symbols) and Požáry (open symbols) intrusions; continuous lines separate plots of different constituents; vertical dashed lines show the position of samples mentioned in the text.

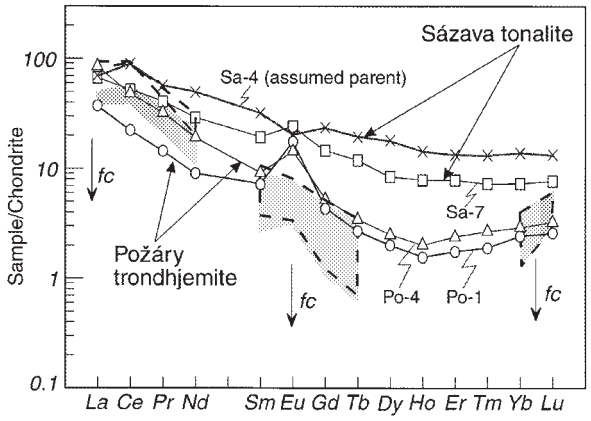

Fig. 9. REE modelling for the Sázava suite; the diagram shows theoretical fields for the liquid composition after 30–40% fractional crystallization (fc) of 52% amphibole, 42% plagioclase, 6% biotite and 0·1% allanite (shaded) and 20–30% fractional crystallization of the same assemblage with 1% apatite and 0·5% titanite instead of allanite (outlined); the distribution coefficients used are given in Table 4.

evolved Sázava tonalite (Sa-4), although without the observed LREE depletion. For this reason, involvement of an additional phase that concentrates LREE, such as allanite or titanite (e.g. Martin, 1987; Sawka, 1988; Evans & Hanson, 1993), both of which occur in the Sázava suite, is necessary. Addition of as little as 0·1% allanite improves the fit of the model (Fig. 9). Were titanite involved in the calculations, a much higher proportion would be needed (0·5%), and 1% apatite would have to be added to compensate for depletion in MREE and HREE. Thus the combined amphibole–plagioclase–allanite model is preferred, although some apatite had to fractionate to account for the gradually decreasing P_2O_5 in the Sázava suite. The origin of strikingly similar REE patterns in trondhjemites from Finland was also explained by fractional crystallization of an amphibole > plagioclase + biotite assemblage from a tonalitic parent (Arth *et al.*, 1978). Drawbacks to this model are (1) the amount of fractionation required by the REE is significantly less than that inferred from the modelling of the Sázava intrusion using major and other trace elements and (2) it fails to reproduce accurately the magnitude of the positive Eu anomaly observed for the trondhjemites. Such discrepancies could be caused by uncertainties in the K_D values for the REE (which, for Eu, is also strongly dependent on the oxygen fugacity), as well as additional processes, such as interaction with basic melts.

Although the slightly peraluminous nature of the trondhjemite can be accounted for by the fractional crystallization model, as peraluminous granitoids can be produced by extensive fractionation of a metaluminous mineral (such as amphibole) from metaluminous melts, the composition of the trondhjemite is also compatible with a genesis through partial melting of amphibolite with reactions such as amphibole → clinopyroxene + olivine + melt or garnet → clinopyroxene + melt (Miller, 1985). The partial melting of garnet amphibolite or eclogite is capable of generating trondhjemites with low ΣREE, high LREE/HREE and pronounced positive Eu anomalies due to the presence in the residue of amphibole and/or garnet (e.g. Cullers & Graf, 1984). The REE patterns observed in the Požáry trondhjemite resemble those modelled as melts of basaltic parents leaving an amphibolite residue (Hanson, 1980), although at somewhat higher ΣREE.

Apart from direct fractionation from mantle-derived basic rocks, trondhjemites and tonalites can be produced by increasing degrees of partial melting of the same metabasic parent (amphibolite, garnet amphibolite or eclogite; e.g. Rapp *et al.*, 1991). The occurrence of the Sázava suite in the proximity of metabasic roof pendants may support an origin by melting of similar material were these rocks to occur at depth. Hence it is worth considering whether such a link could exist between the Požáry trondhjemite and the Sázava tonalite. For a presumed (garnet–) amphibole residue, Ba, as an incompatible element, would be strongly partitioned into the melt and its concentration therein would sharply decrease with increasing degree of melting. On the other hand, the concentration of compatible elements (Cr, Ni, Co, HREE and Y) in the melt should be buffered at a relatively constant level regardless of the degree of melting. Although there is a sharp decrease in Ba with decreasing SiO_2, the concentrations of the above compatible elements increase in the same direction (see examples in Figs 8–10). Hence the partial melting model would also require different parents for both intrusions. Moreover, in the roof pendants of the CBP, metabasites are associated with metasedimentary material, which would be likely to melt first and so strongly influence the Sr–Nd isotopic signature.

In summary, partial melting of metabasites, partial melting of a mantle source with an isotopic signature close to Bulk Earth, or mixing of magmas derived from both sources gave rise to the most primitive rocks of the Sázava intrusion with subsequent extensive fractional crystallization of mainly amphibole and plagioclase producing the intra-suite variation. Either high degrees of fractionation of the Sázava magma or small degrees of melting of a metabasic source could account for the generation of the Požáry trondhjemites.

Blatná suite

The Blatná suite comprises metaluminous to slightly peraluminous high-K calc-alkaline granodiorites and granites, associated with shoshonitic monzonitic rocks.

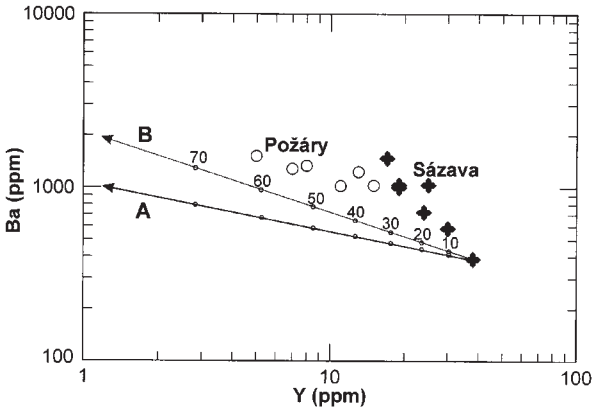

Fig. 10. Ba–Y plot for the Sázava (+) and Požáry (○) intrusions with fractional crystallization vectors calculated for the assemblage obtained from least-squares modelling of major elements (see Table 3 and Fig. 9); numbers refer to percent fractional crystallization. A, both Y and Ba calculated for this assemblage; B, Ba distribution coefficient set to zero (perfectly incompatible behaviour).

The two largest masses within the Blatná suite—the Kozárovice and Blatná intrusions—have been investigated.

Harker variation diagrams (Fig. 11) show strong negative correlations between SiO_2 and FeO*, MnO, MgO, CaO and TiO_2, implying fractionation dominated by ferromagnesian phase(s) and possibly plagioclase. A significant role for biotite and/or K-feldspar is suggested by the negative SiO_2–Ba correlation.

Least-squares calculations (Table 3, Kozárovice assemblage) suggest that the whole compositional spectrum of the Kozárovice intrusion could have been derived by up to ~45% fractional crystallization of 35–42% amphibole, 28–33% plagioclase, 7–13% K-feldspar and 13–22% biotite; this is consistent with the Ba–Sr correlation (Fig. 12). The Kozárovice REE patterns (Fig. 5b) are too uniform for quantitative modelling. However, if the assemblage calculated by the least-squares modelling is considered, the following values of the bulk distribution coefficients (D) are obtained: $D_{La} = 1{\cdot}42$, $D_{Ce} = 1{\cdot}18$, $D_{Eu} = 2{\cdot}48$ and $D_{Lu} = 2{\cdot}01$. For ~40% fractionation, this results in depletions of 10–20% in the LREE, and 40–50% in the MREE and HREE; the Eu anomaly remains nearly constant. The resulting REE pattern falls within the compositional range observed for the Kozárovice intrusion.

The Kozárovice quartz monzonite (KozD-1) may have originated by magma mixing (mingling) between a monzonitic melt and the surrounding granodiorite. This interpretation is supported by microstructural and field evidence such as net-veining of the quartz monzonite, an abundance of mafic microgranular enclaves, and disequilibrium textures in both putative hybrid rocks and the surrounding granodiorite (Janoušek *et al.*, 1997*a*). The mixing test of Fourcade & Allègre (1981) also supports this hypothesis (Fig. 13), suggesting that ~70% of the Kozárovice granodiorite mixed with the monzonite. Small discrepancies in the trace-element composition can be explained either by small-scale fractionation or by lack of information concerning the exact composition of the basic end-member.

The Blatná intrusion is somewhat more evolved than the Kozárovice intrusion (Fig. 11). Least-squares modelling of the intrusion (Table 3, Blatná assemblage) requires up to ~35% fractionation of mainly plagioclase (47–52%), amphibole (17–28%) and biotite (22–31%). This agrees with the Ba–Sr covariations (Fig. 12).

The fact that the content of REE in the less evolved amphibole-rich rocks is significantly higher than in the biotite facies (Fig. 14) implies fractionation of phases with high K_D values for the REE, such as amphibole. On the other hand, the slight decrease in the magnitude of the Eu anomaly (from Eu/Eu* = 0·54–0·67 to 0·70–0·74) is consistent with a roughly balanced influence of feldspar and phases contributing to a positive Eu anomaly in the residual melt (e.g. amphibole, clinopyroxene and apatite). The REE pattern calculated for 20–40% fractionation of the assemblage modelled by major elements and LILE agrees with the available data provided that 0·1% allanite, which is present in these rocks, is introduced into the model to reduce the LREE sufficiently.

Although closed-system fractionation schemes can model successfully the major- and trace-element evolution of the Blatná and Kozárovice intrusions, the linear trends on Harker variation diagrams could also be consistent with a model of magma mixing producing the overall variation within the suite (e.g. Machart, 1992), rather than just on a local scale as discussed above for the Kozárovice quartz monzonite. Furthermore, the variation in initial Sr and Nd isotope ratios (Fig. 6) precludes closed-system behaviour within this suite, and suggests that different sources with distinct isotopic compositions were involved. A simple mixing model between the K-rich monzonites and more evolved members of the Blatná suite can, in theory, account for the observed ($^{87}Sr/^{86}Sr)_{350}$–ε_{Nd}^{350} pattern (Janoušek *et al.*, 1995).

However, on a 1/Nd–ε_{Nd}^{350} plot, the Kozárovice and Blatná intrusions form independent, curved trends (Fig. 15a). Binary mixing as well as AFC (DePaolo, 1981), in which D_{Nd} (bulk distribution coefficient) and r (rate of assimilation/fractional crystallization) are constant, ought to produce linear trends in this diagram (Albarède, 1995). Consequently, these two processes are unlikely to have produced the trends shown. However, curved trends can be explained by changing either D_{Nd} or r in the course of the AFC (Powell, 1984). Both cases are modelled here using the slope of two segments of the 1/Nd–ε_{Nd}^{i} curve (Powell, 1984). The formulae used are given in the

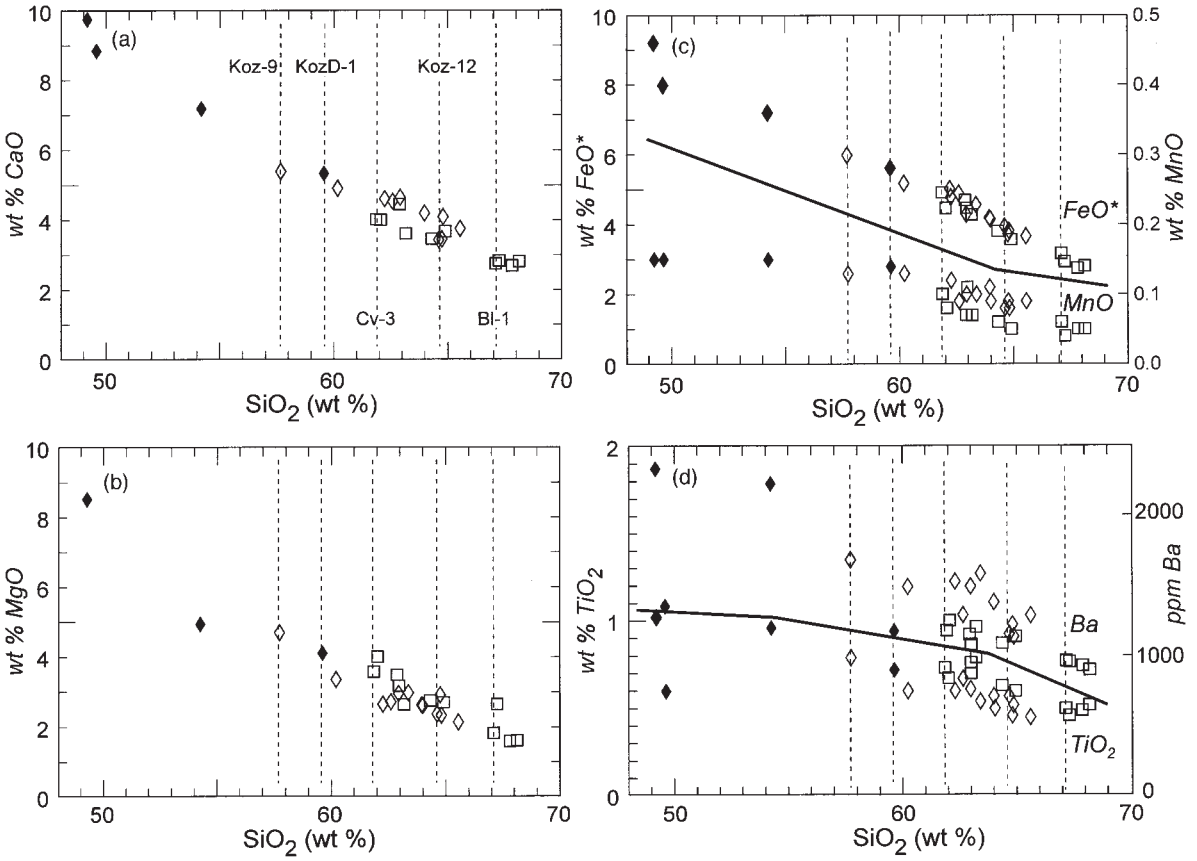

Fig. 11. Variation of silica vs selected major- and trace-element compositions of whole-rock samples from the Blatná (□) and Kozárovice (◇) intrusions, as well as the associated monzonitic rocks (◆); FeO* is total Fe recalculated as FeO; continuous lines separate plots of different constituents; vertical dashed lines show the position of samples mentioned in the text.

Appendix: for the Kozárovice data, these are the Koz-6–Koz-2 and Koz-4–Koz-5 segments, with slopes $S_1 = -695{\cdot}9$ and $S_2 = -24{\cdot}5$, respectively (Fig. 15a). In the following text, subscripts '1' and '2', used to specify r and D, refer to the number of the segment.

(1) Constant D ($D_1 = D_2$), variable r ($r_1 > r_2$)

Such a decrease in r values could possibly reflect a decrease in the temperature of the assimilant encountered by magma ascending through the crust and/or the fact the magma also cools as it crystallizes (see DePaolo, 1981). It should be stressed that this two-step model represents a simplification, as in reality r is likely to change continuously.

Before any assumptions are made about D_{Nd}, r_1 and r_2, a field of possible contaminants can be outlined on the $1/Nd$–ε_{Nd}^{i} plot using equation (6) (see Appendix). For the Kozárovice intrusion, such contaminants could comprise Moldanubian basic granulites and paragneisses (Fig. 15a). The r_1 and r_2 values can be determined by assuming a certain contaminant composition and D_{Nd} [equations (4) and (5)]. Various prospective contaminants were considered using $D_{Nd} = 2{\cdot}3$, calculated for the assemblage given in Table 3 for this intrusion with the addition of 0·1% allanite. For example, the calculation for paragneiss JT-28 results in $r_1 = 2{\cdot}60$ and $r_2 = 0{\cdot}19$.

Although several other assimilants were considered [e.g. more evolved paragneiss CR-5 ($r_1 = 1{\cdot}22$, $r_2 = 0{\cdot}10$) and basic granulite 1059 ($r_1 = 7{\cdot}46$, $r_2 = 0{\cdot}39$)], of the various two-stage AFC curves plotted onto the $(^{87}Sr/^{86}Sr)_{350}$–ε_{Nd}^{350} diagram, that with JT-28 as the contaminant corresponded most closely to the observed variation (Fig. 15b). The influence of uncertainties imposed by the initial choice of D_{Nd} was tested: for $D_{Nd} =$ 2–3 and JT-28 as assimilant, $r_1 =$ 2–4, $r_2 = 0{\cdot}14$–$0{\cdot}29$.

Although using JT-28 as a contaminant provides a satisfactory fit of the data, the resultant r_1 value is unreasonably high (as even the rate of assimilation of hot country rocks is unlikely to exceed the rate of fractional crystallization of the magma, i.e. r should be always lower than about unity: DePaolo, 1981; Taylor & Sheppard, 1986), and so either this model is not feasible, or the contaminant corresponds to an unsampled lithology.

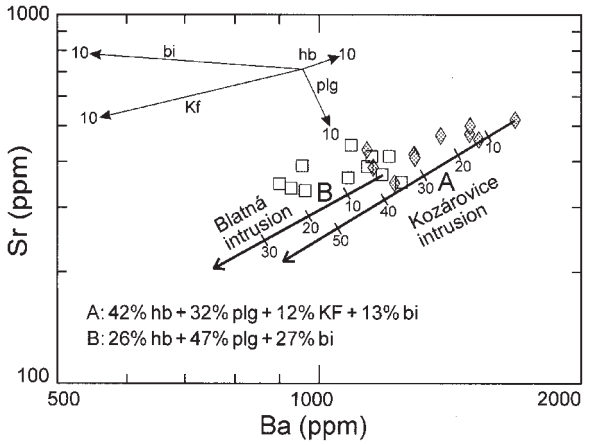

Fig. 12. Ba vs Sr patterns for the Kozárovice (diamonds) and Blatná (squares) intrusions showing the results of trace-element modelling: labelled vectors correspond to 10% fractional crystallization of the main rock-forming minerals, up to 60% fractional crystallization of assemblages A (42% amphibole, 32% plagioclase, 13% biotite and 12% K-feldspar) and B (47% plagioclase, 26% amphibole and 27% biotite) obtained by least-squares modelling of major elements for both intrusions (Table 3); trace-element distribution coefficients used in the modelling are from Hanson (1978) (Table 4).

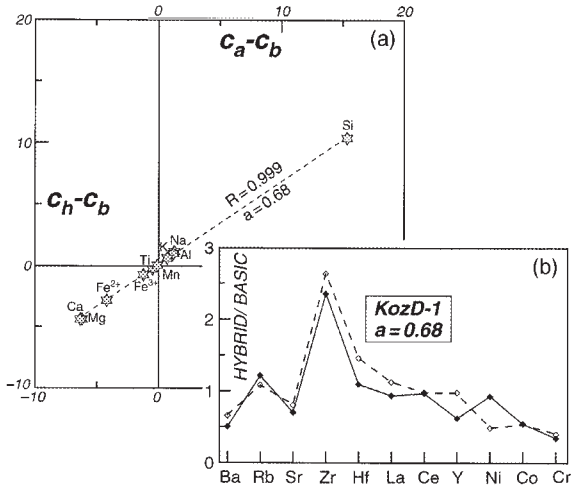

Fig. 13. (a) Major-element based mixing test (Fourcade & Allègre, 1981) for the Kozárovice quartz monzonite; c_a, c_b and c_h correspond to wt % oxide in the acid end-member (Kozárovice granodiorite), basic end-member (monzonite), and suspected hybrid (Kozárovice quartz monzonite), respectively (see Table 1); the slope of the regression line gives the assumed proportion of the acid component *a*. (b) Trace-element mixing test (Castro *et al.*, 1990) that compares the actual trace-element contents in the putative hybrid (continuous line) with theoretical composition of a mixture containing 68% of the acid end-member (dashed line).

For the Blatná intrusion, Fig. 15c suggests that a similar process could have been operative, although with an essentially different parental composition and more restricted field of possible contaminants (almost solely paragneisses). Calculations analogous to those of the

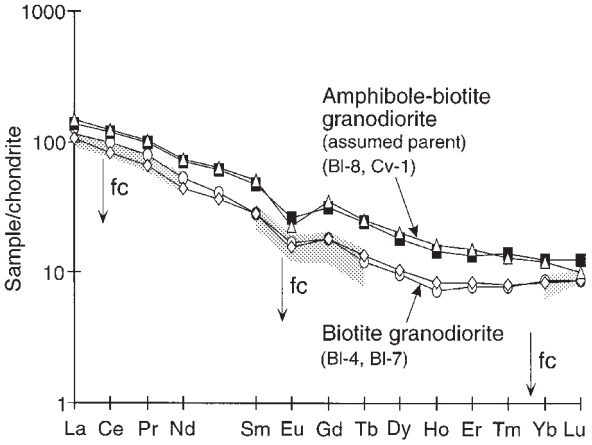

Fig. 14. REE patterns for the Blatná intrusion. Shaded area corresponds to the liquid composition following 20–40% fractional crystallization (fc) of 47% plagioclase, 27% biotite, 26% amphibole and 0·1% allanite.

previous case (first segment Cv-1–Bl-2, second Bl-2–11b, D_{Nd} = 1·81; Fig. 15a) produced comparable results; for assimilant JT-28, the calculated $r_1$and r_2 values were 2·28 and 0·15, respectively. Again, the r_1 value is unreasonably high.

(2) Constant r ($r_1 = r_2$), variable D_{Nd} ($D_1 < D_2$)

As no curved trends are apparent on a plot of $1/Sr$–$(^{87}Sr/^{86}Sr)_{350}$ (not shown), it is assumed that D_{Sr} did not change during crystallization. In the following modelling, D_{Sr} was calculated for the assemblages given in Table 3 for the Kozárovice and Blatná intrusions. However, the curved trends on the $1/Nd$–ε_{Nd}^{350} diagram (Fig. 15d) imply that D_{Nd} and therefore the fractionating assemblage may have changed during the progressive crystallization.

It is difficult to make *a priori* assumptions about possible contaminants for this model [see Appendix, equation (12)]. Both D_1 and D_2 can be determined for a given contaminant composition and r [equations (10) and (11)]. Prospective solutions were tested on the $(^{87}Sr/^{86}Sr)_{350}$–ε_{Nd}^{350} diagram (Fig. 15e). For the Kozárovice data, a good fit was obtained using paragneiss JT-28 as an assimilant and r = 0·5; this resulted in D_1 = 1·25 and D_2 = 4·51, values that are reasonable (see discussion above). This model requires 20–25% fractionation (Fig. 15e and f). The distribution coefficients for the REE are largely controlled by accessory phases; for instance, for the assemblage given in Table 3 for the Kozárovice intrusion, D_{Nd} can be changed from 1·4 to 4·1 by adding as little as 0·3% allanite. The other assimilants (such as granulite 1059 or paragneiss CR-5) failed to reproduce the observed variation in Fig. 15e completely and/or resulted in too high degrees of fractionation.

For the Blatná intrusion, an identical r = 0·5 value was assumed. For the same contaminant, comparable

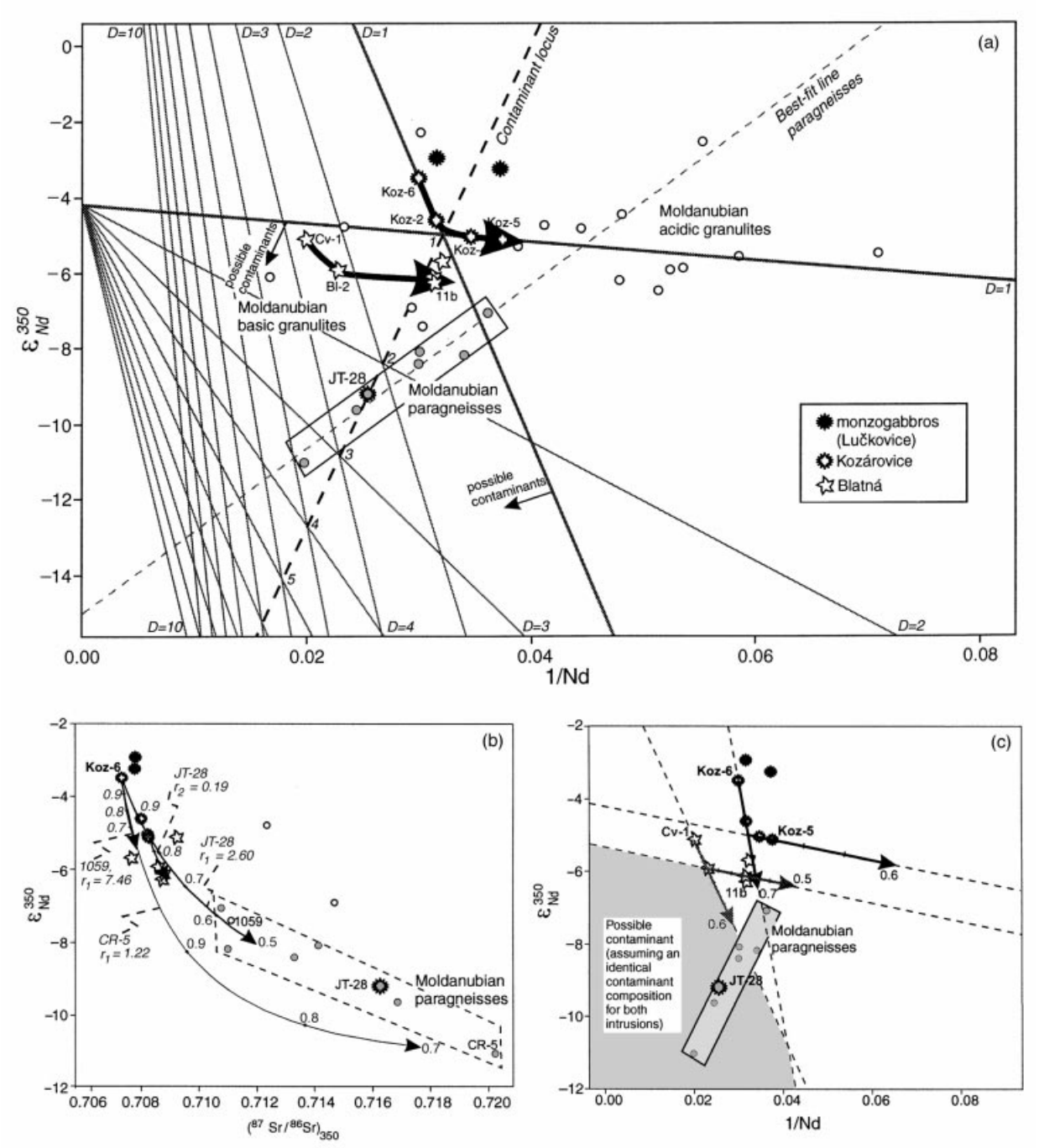

Fig. 15.

bulk distribution coefficients were obtained (D_1 = 1·18, D_2 = 3·66), requiring about 30% AFC (Fig. 15f).

In summary, the geochemical variation shown by the Blatná and Kozárovice intrusions reflects open-system processes, probably AFC with variable D_{Nd} and Moldanubian paragneisses as a contaminant. Moreover, interaction with monzonitic magmas associated with the suite played an important role. The fractionating assemblage was probably dominated by amphibole > plagioclase + K-feldspar > biotite (Kozárovice intrusion) and plagioclase > biotite > amphibole ≫ allanite (Blatná intrusion).

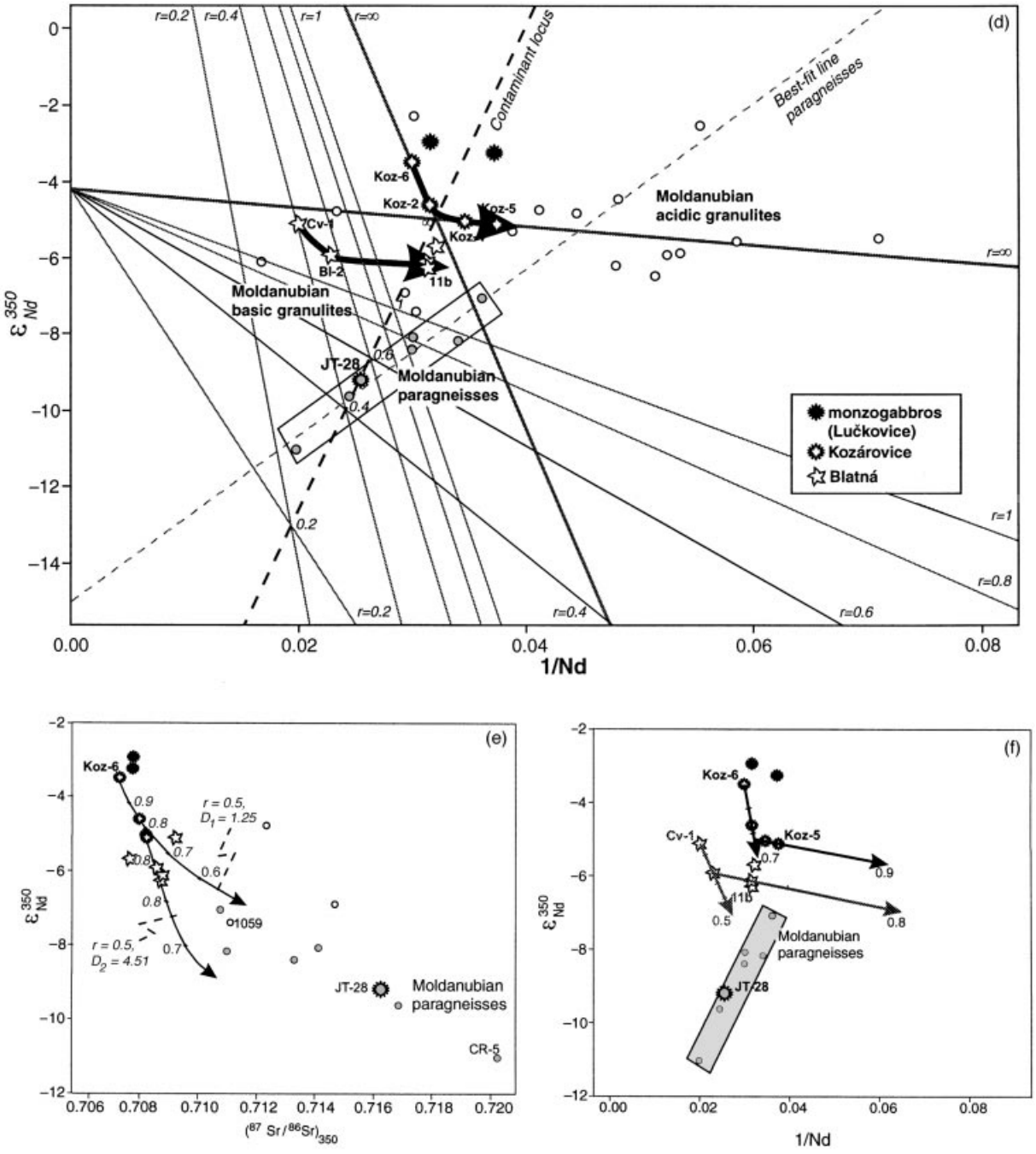

Fig. 15.

Čertovo břemeno suite

The Čertovo břemeno suite is made up of shoshonitic metaluminous to weakly peraluminous melagranites and melasyenites together with minettes. The suite is characterized by high K_2O, P_2O_5, Rb, Zr, Ba and *mg*-number, and low CaO and Na_2O compared with the Sázava and Blatná suites (e.g. Figs 3 and 4; Table 1).

The granitoids of the Čertovo břemeno suite and associated minettes have the most evolved Sr–Nd isotopic compositions within the CBP (Janoušek *et al.*, 1995, 1997*b*). For the minettes, modelling of simple two-component mixing rules out crustal contamination by material isotopically similar to that from the adjacent Moldanubian and Teplá–Barrandian units as the main

mechanism for producing such evolved Sr–Nd compositions. Instead, these are more likely to mirror isotopic compositions of a mantle source that was strongly enriched in incompatible elements (Janoušek *et al.*, 1995, 1997*b*; Holub, 1997). The presence of such a reservoir beneath the Moldanubian unit was recently assumed by Becker (1996) and Gerdes *et al.* (1998). The former worker interpreted garnet pyroxenites from Lower Austria as high-pressure cumulates that crystallized from carbonatite, melilite or lamprophyre magmas. These were shown to be partly contemporaneous with the rocks of the Čertovo břemeno suite, and to have overlapping Sr–Nd isotopic compositions. The origin through melting of a variously enriched lithospheric mantle source was also assumed for Hercynian K-rich rocks elsewhere (Turpin, 1988; Wenzel *et al.*, 1997; Hegner *et al.*, 1998).

Given that the geochemistry of the mafic parts of the Čertovo břemeno suite is similar to that of the minettes, and that the minettes and the more evolved Sedlčany granite have identical Sr–Nd isotopic compositions (Tables 1 and 2), the Sedlčany granite could have originated by closed-system fractional crystallization of a parental, mantle-derived magma corresponding to the mafic members of the suite. The variation in the R_1–R_2 plot points, in theory, to fractionation of Fe-rich biotite, possibly with a significant contribution from K-feldspar and relatively sodic plagioclase (Janoušek, 1994); the Mg-rich composition of the Sedlčany biotite, however, precludes fractionation controlled solely by this mineral. The negative correlation of SiO_2 with Ba and K_2O, and, to some extent, Sr (Fig. 16) is compatible with fractionation of mainly K-feldspar and biotite, whereas a similar trend for CaO suggests a role for amphibole, and/or plagioclase.

Major-element modelling (Table 3) suggests that the SiO_2-rich Sedlčany samples (e.g. Se-12) could have been produced by up to 15–20% fractional crystallization of 30–40% plagioclase, 30–40% K-feldspar, 10–20% biotite and 10–20% amphibole from the SiO_2-poor parts of this intrusion (e.g. Se-6). This model appears to be generally supported by the Ba–Sr plot (Fig. 17); the low degree of fractionation, however, does not allow REE-based modelling.

Some of the variation in the Sedlčany granite could have been caused by assimilation processes that are likely to have been accompanied by fractional crystallization (AFC). In its western part, the granite contains many often partially resorbed xenoliths, especially of carbonates, from the adjacent roof pendants of the Metamorphic Islet Zone. On the other hand, the remarkably uniform Sr–Nd isotopic composition of the granite is not compatible with the operation of extensive assimilation of isotopically different material.

An alternative model has been presented by Holub (1997), who, on the basis of petrography and whole-rock geochemistry, argued that the different members of the suite could have been derived by hybridization of mafic durbachites with leucogranites such as those present within the CBP or the S-type granites such as the Eisgarn intrusion of the Moldanubian Pluton further to the east. Although the similarity in Sr isotopic composition between all these components in the potential mixing process precludes the use of Sr isotopes for assessing the mass balance, it is consistent with such a process (Janoušek *et al.*, 1995; Gerdes *et al.*, 1998).

Taken together, the parental magma of the Sedlčany granite could have been produced either by magma mixing between isotopically similar enriched mantle-derived and leucogranitic components, and/or by fractional crystallization from the Čertovo břemeno parent.

Říčany suite

The Říčany suite comprises peraluminous biotite ± muscovite monzogranites and its petrogenesis has been considered by Janoušek *et al.* (1997*c*). In summary, the evolved, high-level Říčany intrusion is rich in K_2O and Rb, and poor in CaO, MgO and Na_2O, with high Ba/Cs and LREE/HREE, and low K/Rb ratios. The Harker

Fig. 15. AFC modelling for the Blatná suite assuming in (a–c) a constant bulk distribution coefficient (D_{Nd}) and decreasing rate of assimilation/rate of fractional crystallization (r), and in (d–f) a constant r and increasing D_{Nd} (see Table 2 for the data, and text for discussion). (a) $1/Nd–\varepsilon_{Nd}^{350}$ diagram for the Kozárovice intrusion (contaminant: paragneiss JT-28, $D_{Nd} = 2{\cdot}3$), assuming r decreasing from $r_1 = 2{\cdot}60$ to $r_2 = 0{\cdot}19$; two sets of contour lines for variable D are shown, together with their intersections (the contamination locus; Powell, 1984) and the field of possible contaminants calculated using equation (6) (Appendix). (b) $(^{87}Sr/^{86}Sr)_{350}–\varepsilon_{Nd}^{350}$ diagram for the Kozárovice intrusion assuming constant bulk distribution coefficients ($D_{Nd} = 2{\cdot}3$; $D_{Sr} = 2{\cdot}0$) and variable r; modelled trends labelled according to the presumed contaminant (JT-28, CR-5, 1059), r values and decreasing melt fraction (F). (c) $1/Nd–\varepsilon_{Nd}^{350}$ diagram for the Kozárovice and Blatná intrusions (contaminant: JT-28); the bulk distribution coefficient for each intrusion assumed to be constant ($D_{Nd} = 2{\cdot}3$ and $D_{Nd} = 1{\cdot}81$, respectively) and r decreasing from $r_1 = 2{\cdot}60$ to $r_2 = 0{\cdot}19$ (Kozárovice) and $r_1 = 2{\cdot}28$ to $r_2 = 0{\cdot}15$ (Blatná). Labelled vectors correspond to decreasing melt fraction (F). A field of possible contaminants is outlined, assuming an identical contaminant composition for both intrusions. (d) $1/Nd–\varepsilon_{Nd}^{350}$ diagram for the Kozárovice intrusion (contaminant: JT-28, $r = 0{\cdot}5$), assuming D_{Nd} increasing from $D_1 = 1{\cdot}25$ to $D_2 = 4{\cdot}51$; two sets of contour lines for variable r shown, together with their intersection (the contamination locus). (e) $(^{87}Sr/^{86}Sr)_{350}–\varepsilon_{Nd}^{350}$ diagram for the Kozárovice intrusion assuming constant r (0·5), JT-28 as a contaminant, variable D_{Nd} and constant D_{Sr}; modelled trends labelled by D and decreasing melt fraction (F). (f) $1/Nd–\varepsilon_{Nd}^{350}$ diagram for the Kozárovice and Blatná intrusions (contaminant: JT-28); a constant value of $r = 0{\cdot}5$ assumed, and D_{Nd} increasing from $D_1 = 1{\cdot}25$ to $D_2 = 4{\cdot}51$ (Kozárovice) and $D_1 = 1{\cdot}18$ to $D_2 = 3{\cdot}66$ (Blatná); labelled vectors indicate decreasing melt fraction (F).

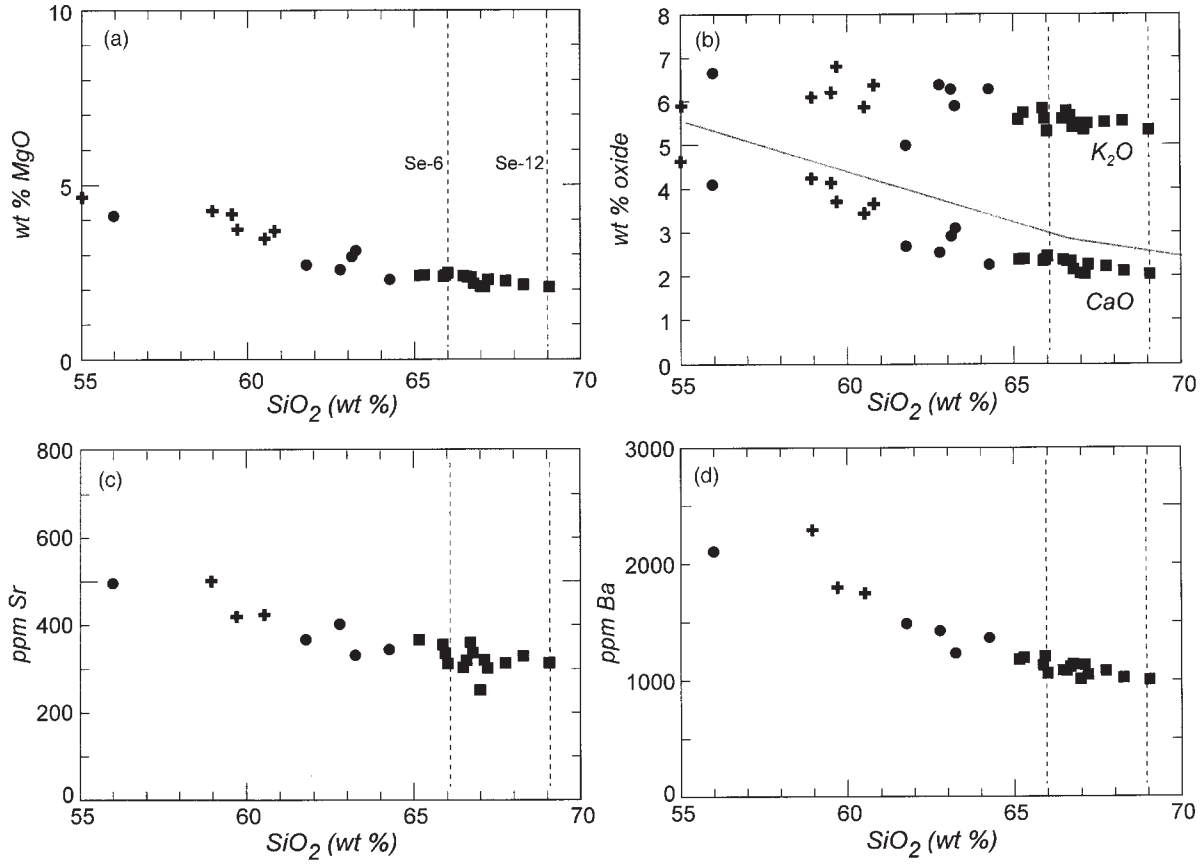

Fig. 16. Binary plots of major- and trace-element compositions of whole-rock samples from Čertovo břemeno suite; +, Tábor; ●, Čertovo břemeno (*s.s.*); ■, Sedlčany.

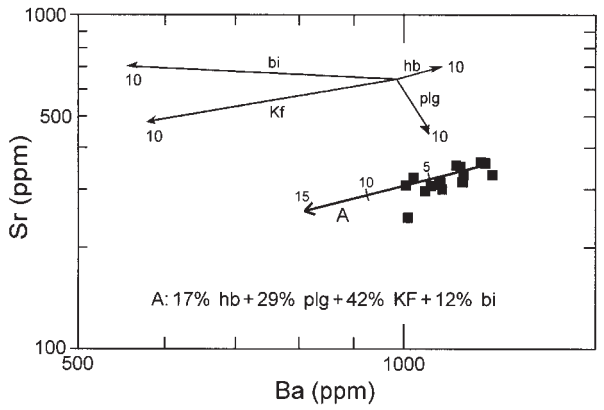

Fig. 17. Sr vs Ba based fractional crystallization modelling for the Sedlčany intrusion: labelled vectors correspond to 10% fractional crystallization of the main rock-forming minerals and up to 10–15% fractional crystallization of the assemblage indicated (see Table 3).

variation diagrams offer little scope for genetic considerations because of the very restricted SiO_2 range, but the R_1–R_2 plot (Fig. 7), together with the observed decrease in Sr and Ba, and increase in Rb, with fractionation are compatible with fractionation controlled by K-feldspar. The intrusion shows cryptic reverse zoning, interpreted as being probably due to rearrangement of a single pulse of magma during intrusion from a vertically graded magma chamber at depth. The whole-rock geochemistry and the Sr–Nd isotopic data are compatible with an origin of the granite by melting of evolved material compositionally similar to the Moldanubian paragneisses or leucocratic granulites.

PETROGENESIS AND GEOTECTONIC SETTING OF THE CENTRAL BOHEMIAN PLUTON

The genesis of granitoids of the CBP has been explained by various models, an overview of which has been given by Holub (1992) and Holub *et al.* (1997*b*). Holub and coworkers, like us, reject granitization models (e.g. Palivcová *et al.*, 1989*a*, 1989*b*; Vlašímský *et al.*, 1992) and conclude that all the intrusions were originally magmas, mobile and capable of inducing thermal metamorphism

on, and being contaminated by, their country rocks. However, it is also clear that any single closed-system process could not have been responsible for generation of the CBP as a whole (e.g. Fig. 6). The geochemical data presented here, together with petrographic and isotopic evidence (e.g. Holub, 1992; Janoušek *et al.*, 1995; Holub *et al.*, 1997*b*) indicate major differences in sources as well as a crucial role for fractional crystallization, AFC and magma mixing–mingling processes in the origin of individual suites. Variously enriched lithospheric mantle played a key role in the petrogenesis of the later suites (Blatná and, in particular, Čertovo břemeno), and the mechanism of mantle enrichment and its geotectonic setting are important aspects to be considered in assessing the development of the CBP.

Role of subduction in the genesis of the CBP

In geotectonic terms, the shift towards K-rich calc-alkaline and shoshonitic granitoid magmatism with time in the CBP may be compatible with a transition from a magmatic-arc to a post-collisional setting (e.g. Holub, 1992). Although the various major- and trace-element based discrimination diagrams do not give unequivocal indications of the tectonic setting of the individual suites (Janoušek, 1994; Holub *et al.*, 1997*b*), the geochemical character of the Sázava suite may point to an origin in a continental arc environment, as suggested especially by its calc-alkaline nature and a pronounced Nb–Ta trough on ocean ridge granite (ORG) normalized multi-element diagrams (Fig. 4).

The operation of subduction in this part of the Bohemian Massif in mid–late Devonian times (~370 Ma) has been inferred from the geochemistry of orthogneisses occurring as roof pendants of the CBP (Košler, 1993). The direct proof of early Hercynian (older than 360 Ma: $^{40}Ar/^{39}Ar$ phengite) subduction-related HP–LT metamorphism in the Bohemian Massif comes from studies of Na amphibole-bearing metabasites, occurring to the NE, in the southeastern Krkonoše Mts (Maluski & Patočka, 1997). Occurrences of similar rocks near the margins of the Saxothuringian zone in the Bohemian Massif may trace a dismembered early Hercynian suture zone (Patočka & Novák, 1997). Petrologically and geochemically analogous, roughly coeval granitoid suites, which occur in the Limousin Tonalite Belt (French Massif Central), the Odenwald, the northern Black Forest, as well as in the Alpine basement, could have been also genetically related to early Hercynian subduction (Shaw *et al.*, (1993); Finger *et al.*, 1997).

Were subduction operative in the area of the CBP early in the development of the Hercynian belt, the mantle wedge above the subduction zone would have been fluxed by LILE-enriched and HFSE-depleted fluids. Tapped at a slightly later stage, this might have promoted melting and the generation of basic calc-alkaline magmas that could have fractionated, and/or provided heat for infracrustal melting to give the more acidic magmas.

This does not, however, imply that subduction was active during the generation of the Sázava suite, as the production of calc-alkaline magmas may post-date the cessation of subduction by as much as 30–50 My (Bonin, 1990). Moreover, as shown above, the majority of the intrusions in the CBP exhibit substantial evidence for mixing of several components. In this plutonic complex, which developed within a relatively short time interval (Holub *et al.*, 1997*a*), the distinct geochemical characteristics of the individual suites do not have to reflect a major change in the geotectonic environment. In this way, the arc-like geochemical signature of both the orthogneisses (Košler, 1993) and the Sázava suite might have been inherited from a source that could itself be arc related. For instance, the metabasic rocks of the adjacent Jílové zone, whose geochemical signature is compatible with that of a potential source for the Sázava suite, were considered to have originated in a late Proterozoic island-arc setting (Waldhausrová, 1984) as supported by the identification of metaboninites therein (Fediuk, 1992).

Mantle enrichment and generation of the basic magmas

A subduction-related volatile influx, regardless of its timing, may have been responsible for widespread variable enrichment of incompatible elements in the local lithospheric mantle, whose later partial melting led to the generation of basic shoshonitic magmas, isotopically similar to the most basic members of the Blatná and Čertovo břemeno suites. A comparable origin for K-rich intrusions occurring in the Elbe valley and Moldanubian zone has been proposed by Wenzel *et al.* (1997).

There are two possible mechanisms of mantle enrichment that could have acted independently or in conjunction with one another.

(1) *In situ* growth of radiogenic Sr and Nd could have followed a single enrichment event that produced a reservoir with a uniform isotopic composition, elevated Rb/Sr and lowered Sm/Nd ratios leading, with time, to higher $^{87}Sr/^{86}Sr$ and lower $^{143}Nd/^{144}Nd$ than in the pre-enrichment source. If melting of the mantle at destructive plate margins does not produce major fractionation of Rb/Sr (Ellam & Hawkesworth, 1988) then, given that the minettes with the highest $(^{87}Sr/^{86}Sr)_{350}$ have $^{87}Rb/^{86}Sr$ of 3–3·5, it would have taken ~170–190 Ma for a source with this $^{87}Rb/^{86}Sr$ to have evolved from an $^{87}Sr/^{86}Sr$ of 0·705 (i.e. similar to the Sázava suite) to 0·712 (i.e.

the initial $^{87}Sr/^{86}Sr$ of the minettes). Thus the enrichment event could have occurred at ~500–550 Ma. As mantle melting leads to a decrease in Sm/Nd in the melt relative to the source, T_{Nd}^{CHUR} model ages can be also used to constrain a minimum age for the enrichment event. For the minettes, these are close to 1·1 Ga (Janoušek *et al.*, 1995). The observed Sr–Nd decoupling may imply that some of the assumptions concerning Sr behaviour were not fulfilled, and that the enrichment is at least Riphean in age. Alternatively, it may point to a direct recycling of a metasedimentary material or mixing of different mantle sources.

(2) Mantle source with an isotopic composition close to, or more depleted than Bulk Earth, could have been contaminated by a subducted metasedimentary component in a manner invoked for the petrogenesis of Hercynian minettes (Turpin *et al.*, 1988) as well as for granitoids from the Sardinia–Corsica Batholith (Tommasini *et al.*, 1995).

The overall range in Sr–Nd isotopic compositions observed in the CBP may have several explanations. The later CBP magmatism could have tapped mantle zones that had a greater subducted sedimentary component, or it could represent lower degrees of partial melting, which preferentially contained the more fusible subducted components. It can be also explained by movement of the melting zone upwards, from the subducted slab to the metasomatized mantle wedge above the fossil subduction zone.

Alternatively, the mixing of distinct mantle components may have taken place. Mafic melts parental to the Sázava suite could have come from a relatively undepleted (asthenospheric?) mantle source, whose upwelling caused heating of the overlying lithospheric mantle. The rise of isotherms would trigger small-scale partial melting of the enriched lithospheric mantle, and lead to contamination during the ascent of the asthenospheric melt, to produce the progressively more enriched basic end-members of the Blatná and Čertovo břemeno suites.

If the lithospheric mantle were geochemically and isotopically heterogeneous, then it was the more enriched zones that were tapped by the later magmatism. The occurrence of K-rich durbachitic rocks exclusively within the Moldanubian unit is consistent with such a heterogeneity having a lateral distribution. The CBP may therefore record the geochemical complexity of processes operating at the boundary between two distinct lithospheric domains (the Teplá–Barrandian and Moldanubian units).

Role of shoshonitic magmas

The heat introduced by the emplacement of shoshonitic magmas into the crust was likely to have been at least partly responsible for widespread crustal anatexis. This anatexis could have been followed by interaction of acidic and shoshonitic magmas, as documented by the abundance of K-rich mafic microgranular enclaves within numerous intrusions of the CBP as well as by petrographic and geochemical evidence for interaction of granodioritic and monzonitic rocks (e.g. Kozárovice quartz monzonite, see above). The modelling of AFC also shows an important role for a crustal contamination in genesis of the Blatná suite.

Taken together, the nearly contemporaneous Blatná and Čertovo břemeno suites (Holub *et al.*, 1997*a*, 1997*b*) may have been generated by mixing of different proportions of variably enriched mantle with a crustal component(s). Such a model resembles that of Harmon *et al.* (1984) and Rock & Hunter (1987) for the genesis of Scottish late Caledonian granitoids in which basic, mantle-derived magmas acted both as parents, undergoing crustal contamination, and as heat sources, facilitating melting.

In the case of the Říčany suite, geochemical and isotopic data are consistent with the input of basic magma into the crust inducing melting of peraluminous lithologies similar to those of the Moldanubian unit. These peraluminous melts did not mix significantly with the basic magmas, and were able to segregate and be emplaced at high crustal levels (Janoušek *et al.*, 1997*c*).

CONCLUSIONS

(1) A diversity of petrogenetic processes is required to account for the geochemical variability shown by the essentially contemporaneous constituent intrusions of the Central Bohemian Pluton.

(2) Partial melting of metabasites, geochemically and isotopically similar to those occurring in the roof pendants of the CBP, partial melting of a mantle source with an isotopic signature close to Bulk Earth, or mixing of magmas derived from both sources gave rise to the relatively primitive calc-alkaline Sázava suite. Geochemical modelling indicates extensive fractional crystallization of mainly amphibole and plagioclase to produce the intra-suite variation. Either high degrees of fractionation of the Sázava magma, or small degrees of melting of a metabasic source could account for the generation of the Požáry trondhjemite.

(3) The variation shown within the mainly granodioritic Blatná suite can be modelled by AFC with a (Moldanubian) paragneiss as a contaminant and increasing D_{Nd} values. The fractionating assemblage is thought to be dominated by amphibole > plagioclase + K-feldspar > biotite (Kozárovice intrusion) and plagioclase > biotite > amphibole ≫ allanite (Blatná intrusion).

(4) Strongly enriched [($^{87}Sr/^{86}Sr)_{350} \sim 0{\cdot}712$, $\varepsilon_{Nd}^{350} \sim -7$) mantle-derived melts that evolved either by closed-system fractional crystallization, or by interaction with leucogranitic magmas, gave rise to the durbachitic Čertovo břemeno suite. The variation in the Sedlčany granite is compatible with small degrees of plagioclase–K-feldspar > biotite–amphibole fractionation, accompanied by limited country-rock assimilation (AFC).

(5) Partial melting of (Moldanubian) metasedimentary lithologies is a likely origin of the granitic rocks of the Říčany suite. The Říčany granite forms a reversely zoned body, whose chemical variation was caused mainly by K-feldspar fractionation at depth before intrusion to a high level.

(6) In the Sázava suite, the basic melts may have provided heat for the crustal melting as well as having mixed and mingled with the tonalitic rocks. Likewise, in the Blatná and Čertovo břemeno suites, the basic melts derived from variously enriched mantle sources have acted both as parents, undergoing crustal contamination, and heat sources, facilitating melting.

(7) Evidence for the operation of subduction during the Hercynian episode in the area of the CBP is equivocal.

(8) There was, with time, a conspicuous shift from a more depleted Sr–Nd isotopic composition and calc-alkaline chemistry towards more evolved K-rich calc-alkaline and shoshonitic rocks, which is interpreted as reflecting the involvement of variously enriched mantle sources in the later suites. Had direct recycling of subducted metasedimentary component into lithospheric mantle been operative, then the subduction could have been as young as mid-Devonian. However, if the radiogenic Sr and unradiogenic Nd composition of the lithospheric mantle was a result of closed-system *in situ* growth, the enrichment event would have been significantly older.

(9) Geochemical study of granitoid suites alone cannot give unambiguous indications of their true geotectonic setting, especially in a context of a complex orogeny such as that of the Hercynides in Central Europe. Instead, the geochemical character may be inherited from the source rocks.

ACKNOWLEDGEMENTS

This work was supported by a University of Glasgow Postgraduate Research Scholarship and Czech Grant Agency Postdoctoral Grant 205/97/P113 (V.J.), both of which are gratefully acknowledged. We are indebted to F. Finger, J. Pearce, U. Schaltegger and M. Wilson for their helpful reviews. We also thank A. Dudek, R. M. Ellam, F. V. Holub, B. E. Leake and W. E. Stephens for discussions and comments; H. Maluski for permission to present unpublished ^{40}Ar–^{39}Ar data; J. Gallagher, V. Gallagher, A. Kelly, R. Macdonald, K. Sampson, T. Shimmield and V. Sixta for technical assistance; and the British Council for funding exchange visits. The work at SURRC was supported by the Scottish Universities.

REFERENCES

Albarède, F. (1995). *Introduction to Geochemical Modelling*. Cambridge: Cambridge University Press.

Arth, J. G., Barker, F., Peterman, Z. E. & Freedman, I. (1978). Geochemistry of the gabbro–diorite–tonalite–trondhjemite suite of southwest Finland and its implications for the origin of tonalitic and trondhjemitic magmas. *Journal of Petrology* **19**, 289–316.

Batchelor, R. A. & Bowden, P. (1985). Petrogenetic interpretation of granitoid rock series using multicationic parameters. *Chemical Geology* **48**, 43–55.

Becker, H. (1996). Crustal trace element and isotopic signatures in garnet pyroxenites from garnet peridotite massifs from Lower Austria. *Journal of Petrology* **37**, 785–810.

Blížkovský, M., Mašín, J., Mátlová, E., Mitrenga, P., Novotný, A., Pokorný, L., Rejl, L. & Šalanský, K. (1992). Linear structures of the Czechoslovak part of the Bohemian Massif based on geophysical data. In: Kukal, Z. (ed.) *Proceedings of the 1st International Conference on the Bohemian Massif*. Prague: Czech Geological Survey, pp. 29–32.

Bonin, B. (1990). From orogenic to anorogenic settings: evolution of granitoid suites after a major orogenesis. *Geological Journal* **25**, 261–270.

Bowes, D. R. & Košler, J. (1993). Geochemical comparison of the subvolcanic appinite suite of the British Caledonides and the durbachite suite of the Central European Hercynides: evidence for associated shoshonitic and granitic magmatism. *Mineralogy and Petrology* **48**, 47–63.

Boynton, W. V. (1984). Cosmochemistry of the rare earth elements: meteoritic studies. In: Henderson, P. (ed.) *Rare Earth Elements Geochemistry*. Amsterdam: Elsevier, pp. 63–114.

Bryan, W. B., Finger, L. W. & Chayes, F. (1969). Estimating proportions in petrographic mixing equations by least-squares approximation. *Science* **163**, 926–927.

Castro, A., De la Rosa, J. D. & Stephens, W. E. (1990). Magma mixing in the subvolcanic environment: petrology of the Gerena interaction zone near Seville, Spain. *Contributions to Mineralogy and Petrology* **105**, 9–26.

Chaloupský, J., Chlupáč, I., Mašek, J., Waldhausrová, J. & Cháb, J. (1995). VII.B.1. Teplá–Barrandian Zone (Bohemicum)—stratigraphy. In: Dallmeyer, R. D., Franke, W. & Weber, K. (eds) *Pre-Permian Geology of Central and Eastern Europe*. Berlin: Springer, pp. 379–391.

Clarke, D. B. (1992). *Granitoid Rocks*. London: Chapman & Hall.

Cullers, R. L. & Graf, J. L. (1984). Rare earth elements in igneous rocks of the continental crust: intermediate and silicic rocks–ore petrogenesis. In: Henderson, P. (ed.) *Rare Earth Elements Geochemistry*. Amsterdam: Elsevier, pp. 275–308.

De la Roche, H., Leterrier, J., Grandclaude, P. & Marchal, M. (1980). A classification of volcanic and plutonic rocks using R_1R_2-diagram and major element analyses—its relationships with current nomenclature. *Chemical Geology* **29**, 183–210.

DePaolo, D. J. (1981). Trace element and isotopic effects of combined wallrock assimilation and fractional crystallization. *Earth and Planetary Science Letters* **53**, 189–202.

Didier, J. & Barbarin, B. (1991). The different types of enclaves in granites—nomenclature. In: Didier, J. & Barbarin, B. (eds) *Enclaves and Granite Petrology*. Amsterdam: Elsevier, pp. 19–24.

Dörr, W., Fiala, J., Franke, W., Haack, U., Philippe, S., Schastok, J., Scheuvens, D., Vejnar, Z. & Zulauf, G. (1998). Cambrian vs. Variscan tectonothermal evolution within the Teplá–Barrandian: evidence from U–Pb zircon ages of syn-tectonic plutons (Bohemian Massif, Czech Republic). *Acta Universitatis Carolinae, Geologica* **42**, 229–230.

Dudek, A. & Fediuk, F. (1957). Basic inclusions and fluidal phenomena in the granodiorite at the border of the Central-Bohemian Pluton near Teletín. *Sborník Ústredního ústavu geologického, oddíl geologický, Slavík's Volume*, 97–112 (in Czech with English summary).

Ellam, R. M. & Hawkesworth, C. J. (1988). Is average continental crust generated at subduction zones? *Geology* **16**, 314–317.

Evans, O. C. & Hanson, G. N. (1993). Accessory-mineral fractionation of rare-earth element (REE) abundances in granitoid rocks. *Chemical Geology* **110**, 69–93.

Fediuk, F. (1992). Metaboninite in the Proterozoic Jílové Belt of Central Bohemia. *Vestník Ústredního ústavu geologického* **67**, 297–310.

Finger, F., Roberts, M. P., Haunschmid, B., Schermaier, A. & Steyer, H. P. (1997). Variscan granitoids of central Europe: their typology, potential sources and tectonothermal relations. *Mineralogy and Petrology* **61**, 67–96.

Fourcade, S. & Allègre, C. J. (1981). Trace elements behavior in granite genesis: a case study. The calc-alkaline plutonic association from the Quérigut Complex (Pyrénées, France). *Contributions to Mineralogy and Petrology* **76**, 177–195.

Gerdes, A., Wörner, G. & Finger, F. (1998). Large chemical variations in the Variscan Rastenberg pluton caused by mixing enriched mantle magmas with crustal melts. *Acta Universitatis Carolinae, Geologica* **42**, 256.

Hanson, G. N. (1978). The application of trace elements to the petrogenesis of igneous rocks of granitic composition. *Earth and Planetary Science Letters* **38**, 26–43.

Hanson, G. N. (1980). Rare earth elements in petrogenetic studies of igneous systems. *Annual Review of Earth and Planetary Sciences* **8**, 371–406.

Harmon, R. S., Halliday, A. N., Clayburn, J. A. P. & Stephens, W. E. (1984). Chemical and isotopic systematics of the Caledonian intrusions of Scotland and Northern England: a guide to magma source region and magma–crust interaction. *Philosophical Transactions of the Royal Society of London, Series A* **310**, 709–742.

Hegner, E., Köbl-Ebert, M. & Loeschke, J. (1998). Post-collisional Variscan lamprophyres (Black Forest, Germany): $^{40}Ar/^{39}Ar$ phlogopite dating, Nd, Pb, Sr isotope and trace element characteristics. *Lithos* **45**, 395–411.

Henderson, P. (1982). *Inorganic Geochemistry*. Oxford: Pergamon Press.

Holub, F. V. (1989). Durbachite. In: Bowes, D. R. (ed.) *The Encyclopaedia of Igneous and Metamorphic Petrology*. New York: Van Nostrand Reinhold, pp. 133–134.

Holub, F. V. (1992). Contribution to petrochemistry of the Central Bohemian Plutonic Complex. In: Soucek, J. (ed.) *Horniny ve vědách o Zemi*. Prague: Charles University, pp. 117–140 (in Czech with English summary).

Holub, F. V. (1997). Ultrapotassic plutonic rocks of the durbachite series in the Bohemian Massif: petrology, geochemistry and petrogenetic interpretation. *Sborník geologických ved, Loziskóvá geologie–mineralogie* **31**, 5–26.

Holub, F. V., Cocherie, A. & Rossi, P. (1997*a*). Radiometric dating of granitic rocks from the Central Bohemian Plutonic Complex (Czech Republic): constraints on the chronology of the thermal and tectonic events along the Moldanubian–Barrandian boundary. *Comptes Rendus de l'Académie des Sciences, Series IIA, Earth and Planetary Sciences* **325**, 19–26.

Holub, F. V., Machart, J. & Manová, M. (1997*b*). The Central Bohemian Plutonic Complex: geology, chemical composition and genetic interpretation. *Sborník geologických ved, Loziskóvá geologie–mineralogie* **31**, 27–50.

Ihaka, R. & Gentleman, R. (1996). R: a language for data analysis and graphics. *Journal of Computational and Graphical Statistics* **5**, 299–344.

Irvine, T. N. & Baragar, W. R. A. (1971). A guide to the chemical classification of common volcanic rocks. *Canadian Journal of Earth Sciences* **8**, 523–548.

Janoušek, V. (1994). Geochemistry and petrogenesis of the Central Bohemian Pluton, Czech Republic. Ph.D. thesis, University of Glasgow.

Janoušek, V., Rogers, G. & Bowes, D. R. (1995). Sr–Nd isotopic constraints on the petrogenesis of the Central Bohemian Pluton, Czech Republic. *Geologische Rundschau* **84**, 520–534.

Janoušek, V., Bowes, D. R., Rogers, G., Farrow, C. M. & Braithwaite, C. J. R. (1997*a*). Microtextural and geochemical evidence for magma hybridization in the genesis of calc-alkaline granitoids. *Journal of the Czech Geological Society* **42**(3), 59.

Janoušek, V., Holub, F. V., Rogers, G. & Bowes, D. R. (1997*b*). Two distinct mantle sources of Hercynian magmas intruding the Moldanubian unit, Bohemian Massif, Czech Republic. *Journal of the Czech Geological Society* **42**(3), 10.

Janoušek, V., Rogers, G., Bowes, D. R. & Vanková, V. (1997*c*). Petrogenesis of a reversely-zoned intrusion: the Říčany granite, Central Bohemian Pluton, Czech Republic. *Journal of the Geological Society, London* **154**, 807–815.

Kodymová, A. & Vejnar, Z. (1974). Accessory minerals in magmatic rocks of the Central Bohemian Pluton. *Sborník geologických ved, Loziskóvá geologie–mineralogie* **16**, 89–123 (in Czech with English summary).

Košler, J. (1993). Age and geochemistry of the Staré Sedlo and Mirotice complexes, Bohemian Massif, Czech Republic. Ph.D. thesis, University of Glasgow.

Košler, J., Aftalion, M. & Bowes, D. R. (1993). Mid–late Devonian plutonic activity in the Bohemian Massif: U–Pb zircon isotopic evidence from the Staré Sedlo and Mirotice gneiss complexes, Czech Republic. *Neues Jahrbuch für Mineralogie, Monatshefte* **1993**, 417–431.

Košler, J., Rogers, G., Roddick, J. C. & Bowes, D. R. (1995). Temporal association of ductile deformation and granitic plutonism: Rb–Sr and $^{40}Ar–^{39}Ar$ isotopic evidence from roof pendants above the Central Bohemian Pluton, Czech Republic. *Journal of Geology* **103**, 711–717.

Machart, J. (1992). Chemical types of granitoids in the southern part of the Central Bohemian Pluton. In: Soucek, J. (ed.) *Horniny ve vedách o Zemi*. Prague: Charles University, pp. 107–116 (in Czech with English summary).

Maluski, H. & Patočka, F. (1997). Geochemistry and $^{40}Ar/^{39}Ar$ geochronology of the mafic metavolcanic rocks from the Rýchory Mountains complex (west Sudetes, Bohemian Massif): palaeotectonic significance. *Geological Magazine* **134**, 703–716.

Martin, H. (1987). Petrogenesis of Archaean trondhjemites, tonalites, and granodiorites from eastern Finland: major and trace element geochemistry. *Journal of Petrology* **28**, 921–953.

Matte, P., Maluski, H., Rajlich, P. & Franke, W. (1990). Terrane boundaries in the Bohemian Massif: result of large-scale Variscan shearing. *Tectonophysics* **177**, 151–170.

Miller, C. F. (1985). Are strongly peraluminous magmas derived from pelitic sources? *Journal of Geology* **93**, 673–689.

Mísař, Z., Dudek, A., Havlena, V. & Weiss, J. (1983). *Geology of Czechoslovakia I, Bohemian Massif*. Prague: SPN (in Czech).

Palivcová, M., Waldhausrová, J. & Ledvinková, V. (1989*a*). Granitisation problem—once again. *Geologický Zborník Geologica Carpathica* **40**, 423–452.

Palivcová, M., Waldhausrová, J. & Ledvinková, V. (1989*b*). Precursors lithology and the origin of the Central Bohemian Pluton (Bohemian Massif). *Geologický Zborník Geologica Carpathica* **40**, 521–546.

Patočka, F. & Novák, J. K. (1997). The Na-bearing metabasites of W Sudetes: dismembered Variscan suture zone in the Bohemian Massif? *Journal of the Czech Geological Society* **42**, 67.

Pearce, J. A., Harris, N. W. & Tindle, A. G. (1984). Trace element discrimination diagrams for the tectonic interpretation of granitic rocks. *Journal of Petrology* **25**, 956–983.

Peccerillo, R. & Taylor, S. R. (1976). Geochemistry of Eocene calc-alkaline volcanic rocks from the Kastamonu area, Northern Turkey. *Contributions to Mineralogy and Petrology* **58**, 63–81.

Powell, R. (1984). Inversion of the assimilation and fractional crystallization (AFC) equations; characterization of contaminants from isotope and trace element relationships in volcanic suites. *Journal of the Geological Society, London* **141**, 447–452.

Pratt, J. P. (1894). On the determination of ferrous iron in silicates. *American Journal of Science* **48**, 149–151.

Rapp, R. P., Watson, E. B. & Miller, C. F. (1991). Partial melting of amphibolite/eclogite and the origin of Archean trondhjemites and tonalites. *Precambrian Research* **51**, 1–25.

Rock, N. M. S. & Hunter, R. H. (1987). Late Caledonian dyke-swarms of northern Britain: spatial and temporal intimacy between lamprophyric and granitic magmatism around the Ross of Mull pluton, Inner Hebrides. *Geologische Rundschau* **76**, 805–826.

Rollinson, H. R. (1993). *Using Geochemical Data: Evaluation, Presentation, Interpretation*. Harlow, UK: Longman.

Saunders, A. D., Norry, M. J. & Tarney, J. (1991). Fluid influence on the trace element compositions of subduction zone magmas. In: Tarney, J., Pickering, K. T., Knipe, R. J. & Dewey, J. F. (eds) *The Behaviour and Influence of Fluids in Subduction Zones*. London: The Royal Society, pp. 151–166.

Sawka, W. N. (1988). REE and trace element variations in accessory minerals and hornblende from the strongly zoned McMurry Meadows Pluton, California. *Transactions of the Royal Society of Edinburgh: Earth Sciences* **79**, 157–168.

Shaw, A., Downes, H. & Thirlwall, M. F. (1993). The quartz-diorites of Limousin: elemental and isotopic evidence for Devono-Carboniferous subduction in the Hercynian belt of the French Massif Central. *Chemical Geology* **107**, 1–18.

Taylor, H. P., Jr & Sheppard, S. M. F. (1986). Igneous rocks: I. Processes of isotopic fractionation and isotope systematics. In: Valley, J. W., Taylor, H. P., Jr & O'Neil, J. R. (eds) *Stable Isotopes in High Temperature Geological Processes. Mineralogical Society of America, Reviews in Mineralogy* **16**, 227–271.

Tommasini, S., Poli, G. & Halliday, A. N. (1995). The role of sediment subduction and crustal growth in Hercynian plutonism: isotopic and trace element evidence from the Sardinia–Corsica Batholith. *Journal of Petrology* **36**, 1305–1332.

Turpin, L., Velde, D. & Pinte, G. (1988). Geochemical comparison between minettes and kersantites from the Western European Hercynian orogen: trace element and Pb–Sr–Nd isotope constraints on their origin. *Earth and Planetary Science Letters* **87**, 73–86.

Vernon, R. H. (1991). Interpretation of microstructures of microgranitoid enclaves. In: Didier, J. & Barbarin, B. (eds) *Enclaves and Granite Petrology*. Amsterdam: Elsevier, pp. 277–291.

Vlašímský, P., Ledvinková, V., Palivcová, M. & Waldhausrová, J. (1992). Relict stratigraphy and the origin of the Central Bohemian Pluton. *Casopis pro mineralogii a geologii* **37**, 31–44 (in Czech with English summary).

Waldhausrová, J. (1984). Proterozoic volcanites and intrusive rocks of the Jílové zone in Central Bohemia. *Krystalinikum* **17**, 77–97.

Wenzel, T., Mertz, D. F., Oberhänsli, R. & Becker, T. (1997). Age, geodynamic setting and mantle enrichment processes of a K-rich intrusion from the Meissen massif (northern Bohemian massif) and implications for related occurrences from the mid-European Hercynian. *Geologische Rundschau* **86**, 556–570.

White, A. J. R. & Chappell, B. W. (1988). Some supracrustal (S-type) granites of the Lachlan Fold Belt. *Transactions of the Royal Society of Edinburgh: Earth Sciences* **79**, 169–181.

APPENDIX: EQUATIONS FOR CURVED AFC TRENDS IN 1/Sr–($^{87}Sr/^{86}Sr)_i$ OR 1/Nd–ε_{Nd}^i DIAGRAMS

The following equations characterize curved trends in diagrams of the reciprocal of trace-element concentration versus the initial isotopic composition, formed as a result of changes in either r (rate of assimilation/rate of fractional crystallization)or D (bulk distribution coefficient) during AFC (see Powell, 1984). The numerical calculations were performed using beta version of the R package for Windows 95 (Ihaka & Gentleman, 1996).

Given two segments of the curve, each of which can be approximated by straight lines of slopes S_1 and S_2, we consider the following cases.

D constant, *r* variable (*r* >0)

r_1, r_2 *assumed, unknown assimilant composition*

For the parameters of the first segment of the data curve (S_1, c_1^i) and for an assumed value of r_1, for each given value of D, we can calculate a straight line on which the contaminant has to reside [Powell, 1984, equation (9)]:

$$I = S_1\left(\frac{r_1 - 1 + D}{r_1}\right)\frac{1}{c} + I_1^i - \frac{S_1}{c_1^i} \qquad (1)$$

where S is slope, D is bulk distribution coefficient, r is rate of assimilation/rate of fractional crystallization, I is isotopic ratio, c is concentration of the element, I^i is initial isotopic ratio, and c^i is initial concentration; subscripts refer to the number of the segment.

We can write an analogous equation for the second segment of the curve:

$$I = S_2\left(\frac{r_2 - 1 + D}{r_2}\right)\frac{1}{c} + I_2^i - \frac{S_2}{c_2^i}. \qquad (2)$$

For a given D value, straight lines calculated according to equations (1) and (2) intersect at a point—the contaminant composition for the given D, r_1 and r_2.

By choosing other values of D, we can produce a series of pairs of lines, the intersections of which can be joined to form a straight line. This corresponds to the contamination locus of Powell (1984) for any value of D and chosen r_1 and r_2 (i.e. the contaminant must lie along this trend).

This trend may be also obtained by equating equations (1) and (2) for D to obtain the composition of the assimilant (c_A, I_A):

$$I_A = \frac{(r_1 - r_2)}{\left(\frac{r_1}{S_1} - \frac{r_2}{S_2}\right)} \frac{1}{c_A} + \left[\frac{\left(I_1^i - \frac{S_1}{c_1^i}\right) r_1 S_2 - \left(I_2^i - \frac{S_2}{c_2^i}\right) r_2 S_1}{r_1 S_2 - r_2 S_1} \right]. \quad (3)$$

D *and assimilant composition assumed, unknown* r_1, r_2

Equations (1) and (2) can be developed into

$$r_1 = \frac{S_1(1-D)}{S_1 + \left(I_1^i - \frac{S_1}{c_1^i} - I_A\right) c_A} \quad (4)$$

and

$$r_2 = \frac{S_2(1-D)}{S_2 + \left(I_2^i - \frac{S_2}{c_2^i} - I_A\right) c_A}. \quad (5)$$

These are analogous to equation (9.4.21) of Albarède (1995).

By dividing equation (4) by equation (5), the $(1 - D)$ terms cancel out, and we obtain the ratio of r_1/r_2, which is independent of D. Having assumed a value of r_1, the value of r_2 is therefore constrained.

Initial constraints on the possible contaminant composition

Important constraints on the contaminant composition are imposed by the fact that r_1, $r_2 > 0$. For instance, if both S_1 and S_2 are negative, and $D > 1$, the denominator must be positive. This is when

$$I_A < S_1 \frac{1}{c_A} + I_1^i - \frac{S_1}{c_1^i} \text{ and } I_A < S_2 \frac{1}{c_A} + I_2^i - \frac{S_2}{c_2^i}. \quad (6)$$

These correspond to the straight-line projections of both segments of the data trend. (Note that they do not depend on either the r_1 or r_2 values, neither on D insofar as $D > 1$.)

r constant (*r* >0), *D* variable

r, D_1, D_2 *assumed, unknown assimilant composition*

Analogous expressions to equations (1) and (2) can be written

$$I = S_1 \left(\frac{r - 1 + D_1}{r} \right) \frac{1}{c} + I_1^i - \frac{S_1}{c_1^i} \quad (7)$$

and

$$I = S_2 \left(\frac{r - 1 + D_2}{r} \right) \frac{1}{c} + I_2^i - \frac{S_2}{c_2^i}. \quad (8)$$

Equating (7) and (8) for r, we can express the contaminant locus as

$$I_A = \frac{S_1 S_2 (D_1 - D_2)}{S_1(D_1 - 1) - S_2(D_2 - 1)} \frac{1}{c_A} + \frac{\frac{S_1 S_2 (D_2 - 1)}{c_1^i} - \frac{S_1 S_2 (D_1 - 1)}{c_2^i} + I_2^i S_1 (D_1 - 1) - I_1^i S_2 (D_2 - 1)}{S_1(D_1 - 1) - S_2(D_2 - 1)}. \quad (9)$$

Again, this corresponds to a straight line in the diagram $1/c$ vs I.

r *and assimilant composition assumed, unknown* D_1, D_2

If the contaminant composition and r value are given, we can calculate D_1 and D_2. Equations (7) and (8) can be developed into

$$D_1 = 1 - \frac{r\left[S_1 + (I_1^i - \frac{S_1}{c_1^i} - I_A) c_A \right]}{S_1} \quad (10)$$

and

$$D_2 = 1 - \frac{r\left[S_2 + (I_2^i - \frac{S_2}{c_2^i} - I_A) c_A \right]}{S_2}. \quad (11)$$

Initial constraints on the possible contaminant composition

Given D_1, $D_2 \geq 0$, $r > 0$, equations (10) and (11) impose constraints on the possible values of c_A, I_A. For instance, assuming S_1, $S_2 < 0$, then

$$\frac{r\left[S_1 + (I_1^i - \frac{S_1}{c_1^i} - I_A) c_A \right]}{S_1} \leq 1$$

and

$$\frac{r\left[S_2 + (I_2^i - \frac{S_2}{c_2^i} - I_A) c_A \right]}{S_2} \leq 1.$$

Therefore

$$I_A \leq \left(S_1 - \frac{S_1}{r}\right)\frac{1}{c_A} + I_1^i - \frac{S_1}{c_1^i}$$

and

$$I_A \leq \left(S_2 - \frac{S_2}{r}\right)\frac{1}{c_A} + I_2^i - \frac{S_2}{c_2^i}. \quad (12)$$

Each of these boundaries represents a fan of straight lines of different slopes, depending on the r values. For $r = +\infty$, they correspond to projections of both segments of the trend. However, for most likely values of r between zero and unity, the slope of these lines changes rapidly from $+\infty$ (vertical; $r = 0$) to zero (horizontal; $r = 1$). Thus the field of possible contaminants becomes infinitely large as r approaches zero. Therefore, these equations are of little practical value for delimiting *a priori* the field of possible contaminants.